Cell

Forkhead Transcription Factors Establish Origin Timing and Long-Range Clustering in *S. cerevisiae*

Simon R.V. Knott,[1,3] Jared M. Peace,[1] A. Zachary Ostrow,[1] Yan Gan,[1] Alexandra E. Rex,[1] Christopher J. Viggiani,[1,4] Simon Tavaré,[1,2] and Oscar M. Aparicio[1,*]

[1]Molecular and Computational Biology Program, University of Southern California, Los Angeles, CA 90089, USA
[2]Department of Oncology, University of Cambridge, UK
[3]Present address: Cold Spring Harbor Laboratory, Cold Spring Harbor, NY 11724, USA
[4]Present address: Department of Molecular Biology and Genetics, The Johns Hopkins University School of Medicine, Baltimore, Maryland 21205, USA
*Correspondence: oaparici@usc.edu
DOI 10.1016/j.cell.2011.12.012

SUMMARY

The replication of eukaryotic chromosomes is organized temporally and spatially within the nucleus through epigenetic regulation of replication origin function. The characteristic initiation timing of specific origins is thought to reflect their chromatin environment or sub-nuclear positioning, however the mechanism remains obscure. Here we show that the yeast Forkhead transcription factors, Fkh1 and Fkh2, are global determinants of replication origin timing. Forkhead regulation of origin timing is independent of local levels or changes of transcription. Instead, we show that Fkh1 and Fkh2 are required for the clustering of early origins and their association with the key initiation factor Cdc45 in G1 phase, suggesting that Fkh1 and Fkh2 selectively recruit origins to emergent replication factories. Fkh1 and Fkh2 bind Fkh-activated origins, and interact physically with ORC, providing a plausible mechanism to cluster origins. These findings add a new dimension to our understanding of the epigenetic basis for differential origin regulation and its connection to chromosomal domain organization.

INTRODUCTION

Chromatin structure and organization influence most every genomic process (Jenuwein and Allis, 2001; Misteli, 2007). Modification of chromatin structure to accommodate one genomic task inevitably alters the landscape for other processes. To function concurrently, fundamental processes such as DNA replication and transcription must be coordinated to preserve the accuracy and integrity of both, failure of which may lead to genome instability and developmental defects (Gondor and Ohlsson, 2009; Hiratani et al., 2009; Knott et al., 2009a; Mechali, 2010). Epigenetic regulation of replication origin activation is thought to play a role in coordinating DNA replication with other genomic tasks, however our current understanding of how chromosomal replication is regulated by chromatin, let alone organized in three dimensions, is mostly correlative and sparse on mechanism.

Chromosomal DNA replication is governed primarily through regulation of replication initiation at origins. Origin DNA binds ORC and these are joined, in G1 phase, by inactive MCM helicase complexes resulting in assembly of prereplicative complexes (pre-RCs), which are competent to initiate replication. Upon S phase entry, Dbf4-dependent kinase (DDK) stimulates the loading of Cdc45 and Cyclin-dependent kinase stimulates the loading of additional factors to convert pre-RCs into active replisomes (Bell and Dutta, 2002). However, not all pre-RCs initiate replication synchronously at the onset of S phase, nor do all potential origins fire in every cell across a population. Instead, a subset of pre-RCs initiates replication early while clustering into foci, each containing multiple replisomes, that constitute replication factories (Kitamura et al., 2006; Meister et al., 2007). The dynamic nature of the replication foci suggests that as early replicons terminate, these factories are disassembled, allowing the next subset(s) of pre-RCs to initiate replication and establish new factories (Sporbert et al., 2002). The process is not purely stochastic. Whether in yeast or mammalian cells, certain origins reproducibly initiate more efficiently (i.e., the frequency of initiation per cell cycle, ≤ 1) and/or earlier than others (across a population of cells), thereby giving rise to characteristic replication timing patterns of chromosomes (Diller and Raghuraman, 1994; Weinreich et al., 2004).

Replication timing generally correlates with gene activity and chromatin structure, with earlier replicating regions being transcriptionally active and euchromatic, and later replicating regions being transcriptionally silent and heterochromatic (Gilbert, 2002; Gondor and Ohlsson, 2009; MacAlpine and Bell, 2005; Mechali, 2010; Weinreich et al., 2004). These correlations suggest that origins may be subject to similar modes of regulation by local chromatin structure as promoters. Indeed, transcription factors can stimulate origin activity (Chang et al., 2004; Danis et al., 2004; Marahrens and Stillman, 1992), and

active origins frequently colocalize with transcription start sites of active genes in *Drosophila* and mammalian cells (Cadoret et al., 2008; Karnani et al., 2010; MacAlpine et al., 2010; Sequeira-Mendes et al., 2009). The role of transcription factors here is thought to involve the recruitment of chromatin remodelers or modifiers that position nucleosomes or otherwise increase accessibility of origins to *trans*-acting factors (Flanagan and Peterson, 1999; Hu et al., 1999; Li et al., 1998; Lipford and Bell, 2001). Similar to their effects on transcription, local histone deacetylation typically delays or suppresses origin firing, whereas histone acetylation advances or stimulates origin activity (Aggarwal and Calvi, 2004; Aparicio et al., 2004; Goren et al., 2008; Knott et al., 2009c; Pappas et al., 2004; Stevenson and Gottschling, 1999; Vogelauer et al., 2002; Weber et al., 2008). However, distinct aspects of chromatin structure may affect origin timing versus efficiency. Recent studies indicate that histone acetylation is required for pre-RC assembly (Miotto and Struhl, 2007), and multiple, acetylated lysines in histone H3 and H4 N-termini are required for efficient origin activity (Eaton et al., 2011; Unnikrishnan et al., 2010). The mechanism of temporal control is less clear. Early firing is thought to represent a default state, with deacetylated chromatin imposing a delay.

Recently, we reported that the Rpd3L histone deacetylase delays the activation of ~100 origins throughout the yeast genome (~1/3 of the active origins) (Knott et al., 2009c). With this dataset we used classification-regression trees to identify annotated protein binding-sites (from Harbison et al., 2004) whose presence or absence near origins was predictive of origin regulation by Rpd3L. This and further analysis identified binding sites of Forkhead transcription factors, Fkh1 and Fkh2, as being depleted near Rpd3L-regulated origins (data not shown). Fkh1 and Fkh2 have been well characterized for their role in regulating G2/M phase specific transcription of a group of genes known as the *CLB2* cluster (Murakami et al., 2010), but have no known role in DNA replication. In this study, we show that Fkh1 and Fkh2 regulate the initiation timing of most of the earliest origins in the yeast genome through a novel mechanism involving origin clustering in G1 phase.

RESULTS

Fkh1 and Fkh2 Control Genome-wide Initiation Dynamics of Replication Origins

To test whether Fkh1 and Fkh2 influence replication origin function, we examined genome-wide origin-firing using BrdU immunoprecipitation analyzed by DNA sequencing (BrdU-IP-Seq), in cells arrested in early S phase with hydroxyurea (HU). In this analysis, BrdU peak size is proportional to origin efficiency in HU: early-efficient origins produce large peaks while late and/or dormant origins yield smaller or no peaks (Knott et al., 2009c). Because Fkh1 and Fkh2 play partially complementary yet opposing roles in regulation of G2/M phase regulated genes (Murakami et al., 2010), we analyzed single as well as double-deletion mutants of *FKH1* and *FKH2*. Furthermore, because the double mutant cells exhibit slow, pseudohyphal growth, which complicates their analysis, we also examined these cells with overexpression of C-terminally truncated *FKH2* (+*pfkh2ΔC*), which largely restores *CLB2* cluster gene regulation (Reynolds et al., 2003). Consistent with this, we found that expression of Fkh2ΔC in *fkh1Δfkh2Δ* cells suppressed their pseudohyphal growth and restored nearly normal growth rate (Figure S1A, available online, and data not shown).

In wild-type (WT) cells, 295 peaks of BrdU incorporation were detected genome-wide (Figure 1A and Data S1). Combined deletion of *FKH1* and *FKH2* had an unprecedented effect on origin activity throughout the genome, with the activities of the archetypal early origins *ARS305* and *ARS607* being strongly reduced (Figure 1A). Genome-wide, of the 352 origins that were detected to fire in WT and/or *fkh1Δfkh2Δ* cells, 106 (30%) origins were significantly decreased in activity (Fkh-activated) and 82 (23%) were significantly increased (Fkh-repressed) (Table S1 and Data S1). Deletion of *FKH1* significantly (FDR < 0.005) altered the activity of specific origins, with 35 being Fkh-activated and 16 Fkh-repressed, whereas deletion of *FKH2* had no significant effect on the replication pattern (Figure 1A, Figures S1B and S1C, Table S1, and Data S1). Fortuitously, expression of *fkh2ΔC*, while complementing the pseudohyphal growth defects due to transcriptional deregulation, did not complement the origin deregulation of *fkh1Δfkh2Δ* cells, with virtually all of the same origins being identified as Fkh-activated (95) or Fkh-repressed (80) (Figure 1A, Figures S1B and S1C, Table S1, and Data S1). This result demonstrates that the C terminus of Fkh2 is required for origin regulation, and suggests that the effects on origins are independent of transcriptional regulation by Fkh1 and Fkh2. We took advantage of the ability of *fkh2ΔC* expression to complement the transcriptional defects, but not the replication defects, and to improve the growth of the double mutant cells to facilitate further analyses of *fkh1Δfkh2Δ* cells.

Two-dimensional clustering of the Fkh-regulated origins based on their peak sizes allows a global comparison of origin activities in the WT, single and double mutant strains. This analysis reveals the extensive deregulation of *fkh1Δfkh2Δ* and *fkh1Δfkh2Δ +pfkh2ΔC* cells, the strong similarity between replication patterns in the WT and *fkh2Δ* cells, and the intermediate phenotype of *fkh1Δ* cells (Figure 1B). These data indicate that Fkh1 and Fkh2 play a major and complementary role in selecting certain origins for early activation, while repressing the activation of others. Fkh1 is sufficient to maintain normal (early) origin regulation in the absence of Fkh2, whereas Fkh2 only partially compensates for the absence of Fkh1.

To appraise the global relationship between origin activities and regulation by Fkh1 and/or Fkh2 (Fkh1/2), we arranged origins according to their WT activity levels (in HU) and plotted the positions of Fkh-activated and -repressed origins (Figure 1C). Fkh-activated origins were strongly enriched among earlier-firing origins while Fkh-repressed origins were strongly enriched among later-firing (or inefficient) origins ($p < 0.001$, hypergeometric test). These results show that Fkh1 and Fkh2 are largely responsible for differential origin firing dynamics throughout the genome.

To examine in more detail the effect of Fkh1 and Fkh2 on temporal origin-firing dynamics, we analyzed replication throughout an unperturbed, synchronous S phase. Total DNA content analysis showed similar overall replication kinetics in WT and *fkh1Δfkh2Δ +pfkh2ΔC* cells (hereon *fkh1Δfkh2ΔC*)

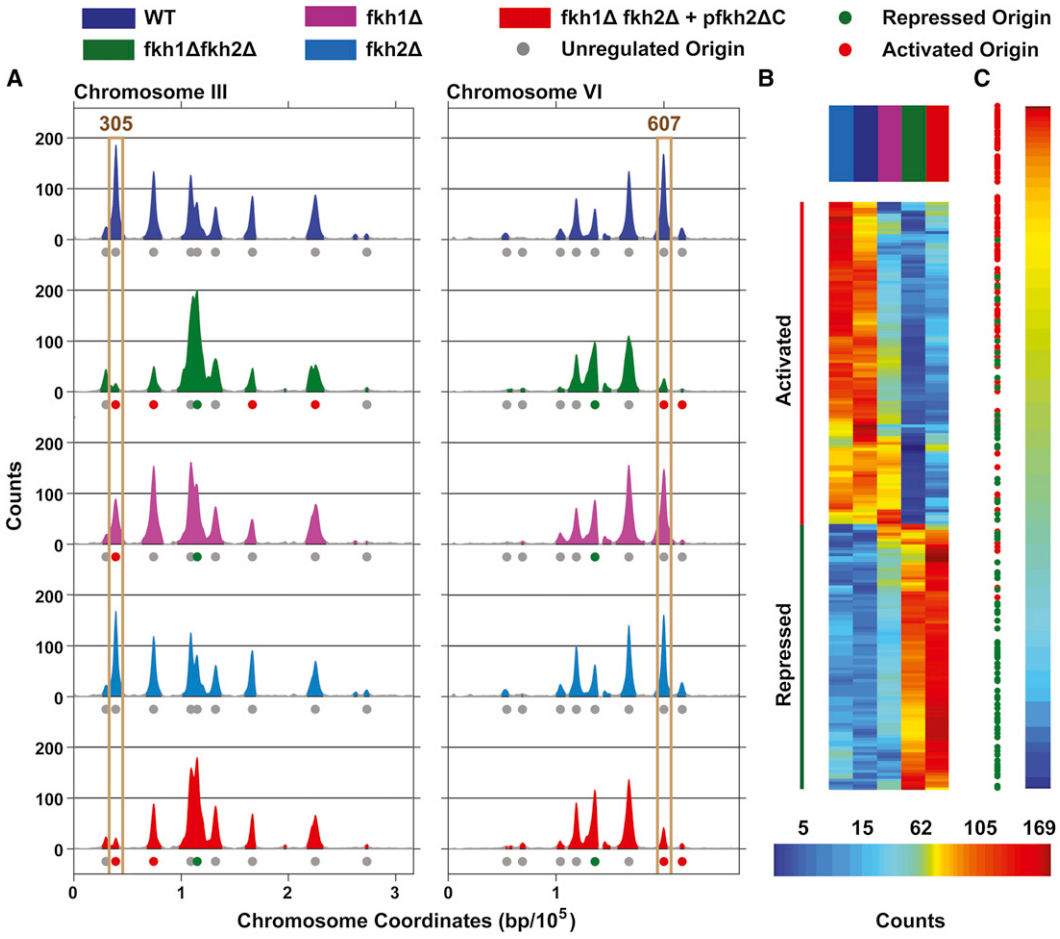

Figure 1. Analysis of Early S Phase BrdU Incorporation

(A) BrdU incorporation plots of chromosomes III and VI are shown; plot colors and symbols correspond to the strain key above. Origins discussed in the text are boxed.

(B) Two-dimensional clustering of peak counts at Fkh-regulated origins is shown; columns (color-keyed above) correspond to strains and rows to origins.

(C) All detected origins (in rows) are arranged from maximum to minimum counts in WT, with the positions of Fkh-regulated origins indicated.

See also Figure S1, Table S1, and Data S1.

(Figure S2A). We next used BrdU pulse labeling combined with BrdU-IP analyzed by microarray (BrdU-IP-chip) to analyze origin-firing dynamics. At Fkh-activated *ARS305* in WT cells, substantial BrdU incorporation occurred during the 12–24 min through 30–42 min pulses, and ceased by the 36–48 min pulse, consistent with the early and synchronous replication of this origin (Figure 2A). In *fkh1Δfkh2ΔC* cells, however, BrdU incorporation at *ARS305* was delayed and reduced in comparison, occurring mainly after replication had ceased in the WT (Figure 2A). *ARS607* and numerous other early origins showed similar delay of activity in *fkh1Δfkh2ΔC* cells (Data S2). These data confirm the results of the analysis with HU and demonstrate that Fkh1/2 are required for the early activation of many origins throughout the yeast genome.

The data also indicate that Fkh1/2 normally repress the earlier firing of many origins (Data S2). For example, examination of the late-replicating region of chromosome XV demonstrates that several later-firing origins, such as *ARS1520*, initiated replication earlier in the mutant cells (Figure 2A). To address the formal possibility that the observed differences in origin activation timing derive from a change in origin activation efficiency, we performed two-dimensional gel electrophoresis analysis of replication initiation structures of Fkh-activated origin *ARS305* and Fkh-repressed origin *ARS1520*. Both origins exhibit high efficiency in both WT and *fkh1Δfkh2ΔC* cells (Figure S2B). These data confirm that that Fkh1/2 establish the temporal program of origin activation.

For a global view of the impact of Fkh1/2 regulation on the temporal program, we clustered the Fkh-regulated origins according to their peak-count differences in the HU analysis, and plotted the differences in their levels of BrdU-incorporation between WT and mutant for each interval in the time-course (Figure 2B). This analysis shows global correspondence between the change in origin activity in HU and the change in origin activity in the time course in the *fkh1Δfkh2ΔC* cells, with Fkh-activated origins firing earlier and Fkh-repressed origins firing

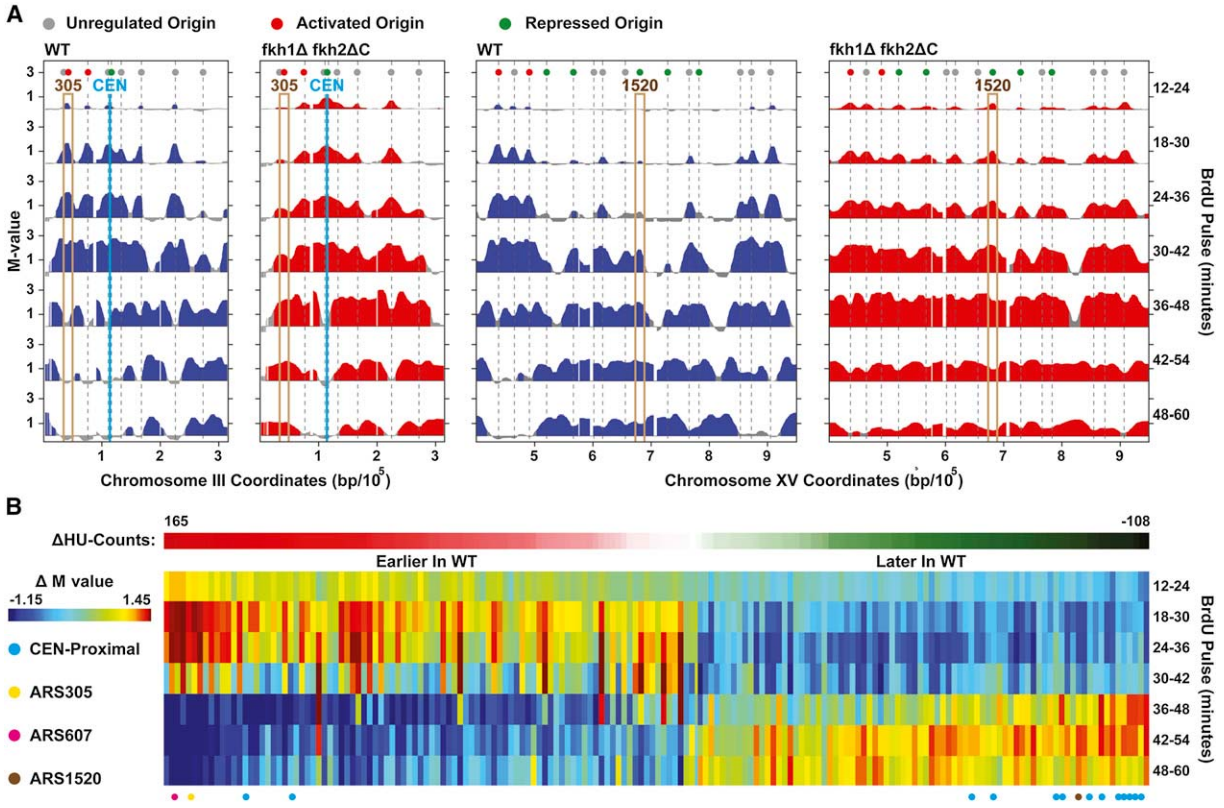

Figure 2. Temporal Analysis of DNA Replication by BrdU Pulse Labeling

(A) BrdU incorporation plots of chromosome III and a region of XV are shown. Origins discussed in the text are boxed.

(B) The matrix shows differences (*WT-fkh1Δfkh2ΔC*) in BrdU incorporation (ΔM value) at all Fkh-regulated origins (columns) across time (rows); the origins are arranged from left to right by their differences (*WT-fkh1Δfkh2ΔC*) in BrdU incorporation in HU (ΔHU Counts). Specific origins are indicated below.

See also Figure S2 and Data S2.

later in WT cells. Thus, Fkh1/2 play a major role in determining the characteristic firing times of replication origins throughout much of the yeast genome.

Fkh Regulation Involves Establishment of Replication-Timing Domains

Comparison of the WT and mutant chromosomal replication profiles reveals additional features of interest, including even earlier replication of centromere (CEN)-proximal sequences, such that these became the earliest replicating region of each chromosome (Figure 2A and Data S2). Plotting CEN-proximal origins (i.e., within 25 kb) in the time-course clustergram shows that many of these origins initiated earlier in the mutant cells and were among the most strongly affected of the Fkh-repressed origins (Figure 2B). Another striking feature of the mutant replication profiles is the delayed replication of most telomere (TEL)-proximal sequences (Data S2), particularly those with active origins, as evident on the right arm of chromosome III (Figure 2A). These results further demonstrate the global role of Fkh1/2 in determining genome replication timing and suggest a function in chromosomal organization.

We wondered whether the distribution of Fkh-regulated origins along chromosomes might provide additional clues about their functional organization. Chromosomal plots of Fkh-regulated origins (ignoring nonregulated origins) show frequent, linearly contiguous groups of Fkh-activated and -repressed origins, suggesting a nonrandom distribution (Figure S2C). To test this notion rigorously, we applied a permutation test that determines the likelihood that the contiguous groups are random. The result shows that the distribution of Fkh-activated and -repressed origins is nonrandom and that origins of each class frequently cluster linearly along the chromosome with other members of their class ($p < 0.01$, Figure S2D). Together with the CEN- and TEL-specific effects, these results are consistent with Fkh1/2 establishing domains of replication timing.

Fkh1/2 Bind and Function in *cis* to Fkh-Activated Origins

Fkh1 and Fkh2 exhibit similar DNA sequence binding specificities in vitro and bind extensively throughout the genome, with significant overlap of binding sites (data not shown and Harbison et al., 2004; Hollenhorst et al., 2001; MacIsaac et al., 2006). To examine the relationship of Fkh1 and Fkh2 binding with origin regulation, we analyzed the distribution of putative Fkh1 and Fkh2 binding sites within 500 bp of Fkh-activated, -repressed, and -unregulated origins (see Experimental Procedures). This analysis shows that Fkh1 and Fkh2 binding sites are enriched

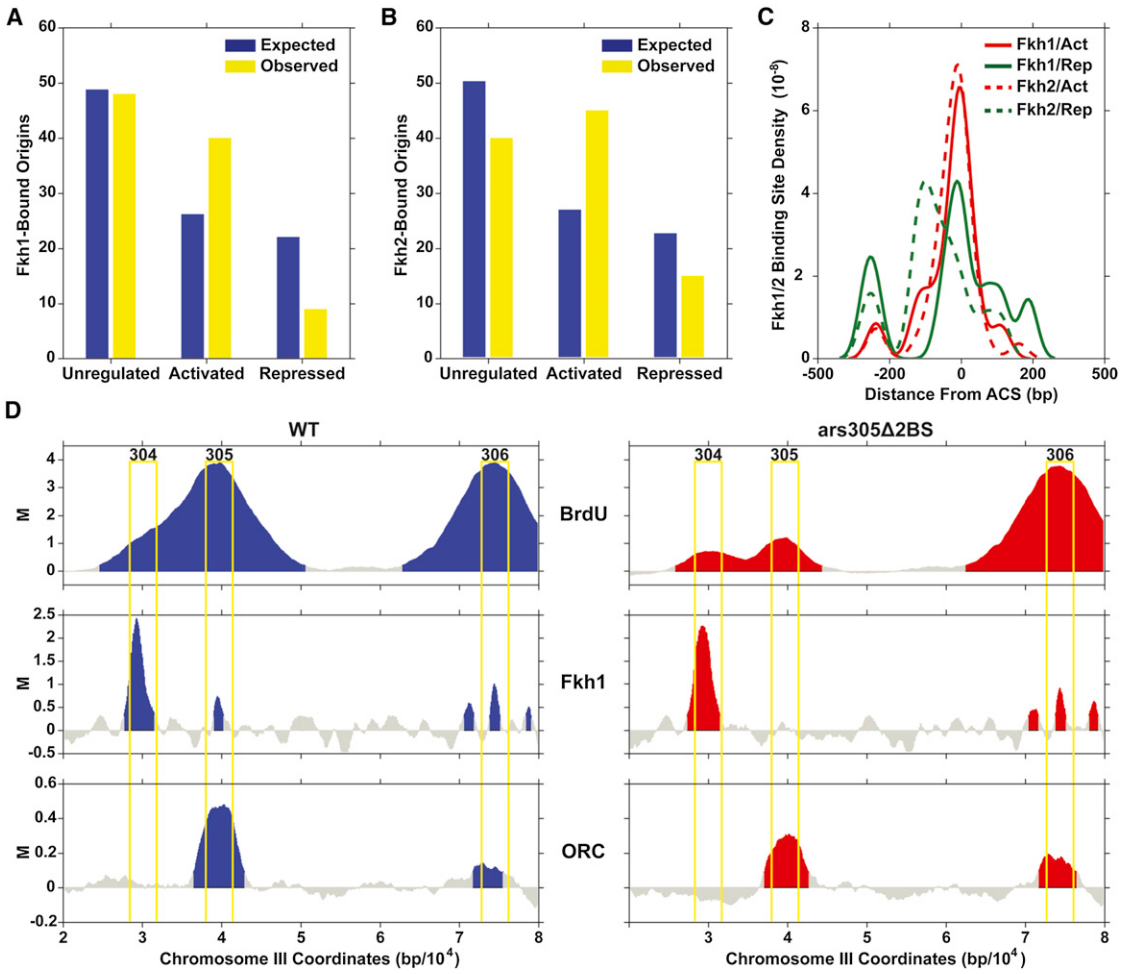

Figure 3. Analysis of Fkh1 and Fkh2 Binding Sites near Origins

(A) and (B) Frequencies of expected and actual Fkh1 (A) and Fkh2 (B) consensus binding sites near Fkh-activated, Fkh-unregulated, and Fkh-repressed origins are shown.

(C) Frequency distribution plots of Fkh1 and Fkh2 consensus binding sites relative to ACS position are shown.

(D) M values for BrdU-IP-chip and for ChIP-chip of Fkh1 and ORC binding along the *ARS305* region in WT cells harboring *ARS305* or *ars305Δ2BS*.

near Fkh-activated origins and depleted near Fkh-repressed origins (Figures 3A and 3B, hypergeometric test, $p < 0.01$), as expected if Fkh1/2 act through direct binding near Fkh-activated origins. Fkh1 was most enriched, being ~4-fold enriched at Fkh-activated versus -repressed origins, consistent with a predominant role for Fkh1 rather than Fkh2 in origin regulation as indicated by the single mutant analysis above.

The enrichment of Fkh1/2 binding sites near origins may explain the selection of these origins for early activation, however, Fkh1/2 bind near some origins that are not Fkh-activated suggesting that Fkh1/2 binding in the vicinity is not sufficient for origin activation. To determine more precisely how Fkh1 and Fkh2 localize in relation to Fkh-regulated origins, we calculated the distance from each origin's *A*RS-consensus *s*equence (ACS), which binds ORC, to the likeliest Fkh1 and Fkh2 binding site within 500 bp and plotted the results as a frequency distribution (see Experimental Procedures). The distribution reveals extraordinary proximity of Fkh1 and Fkh2 consensus sites to ACSs of Fkh-activated origins, with frequent overlap of the Fkh1/2 binding sites and ACSs (Figure 3C). In contrast, Fkh1 and especially Fkh2 showed poorer alignment and binding density with those few Fkh-repressed origins proximal to Fkh1/2 binding sites. These results suggest that the positioning and/or number of these sites may be important for origin regulation.

To test directly whether Fkh1/2 regulate origin function through binding in *cis* to the affected origin, we mutated two putative Fkh1/2 binding sites near *ARS305* (*ars305Δ2BS*). Combined mutation of these sites significantly reduced BrdU incorporation at *ARS305,* but not at more distal origins, indicating that Fkh1/2 regulate *ARS305* directly through binding in *cis* (Figure 3D). Crucially, mutation of these binding sites eliminated Fkh1 binding to the *ARS305* region without eliminating ORC binding (Figure 3D). These results also eliminate concerns that origin deregulation results from mis-expression of a replication factor(s) in *fkh1Δfkh2ΔC* cells. Overall, these results demonstrate that Fkh1/2 binding positively influences origin activity.

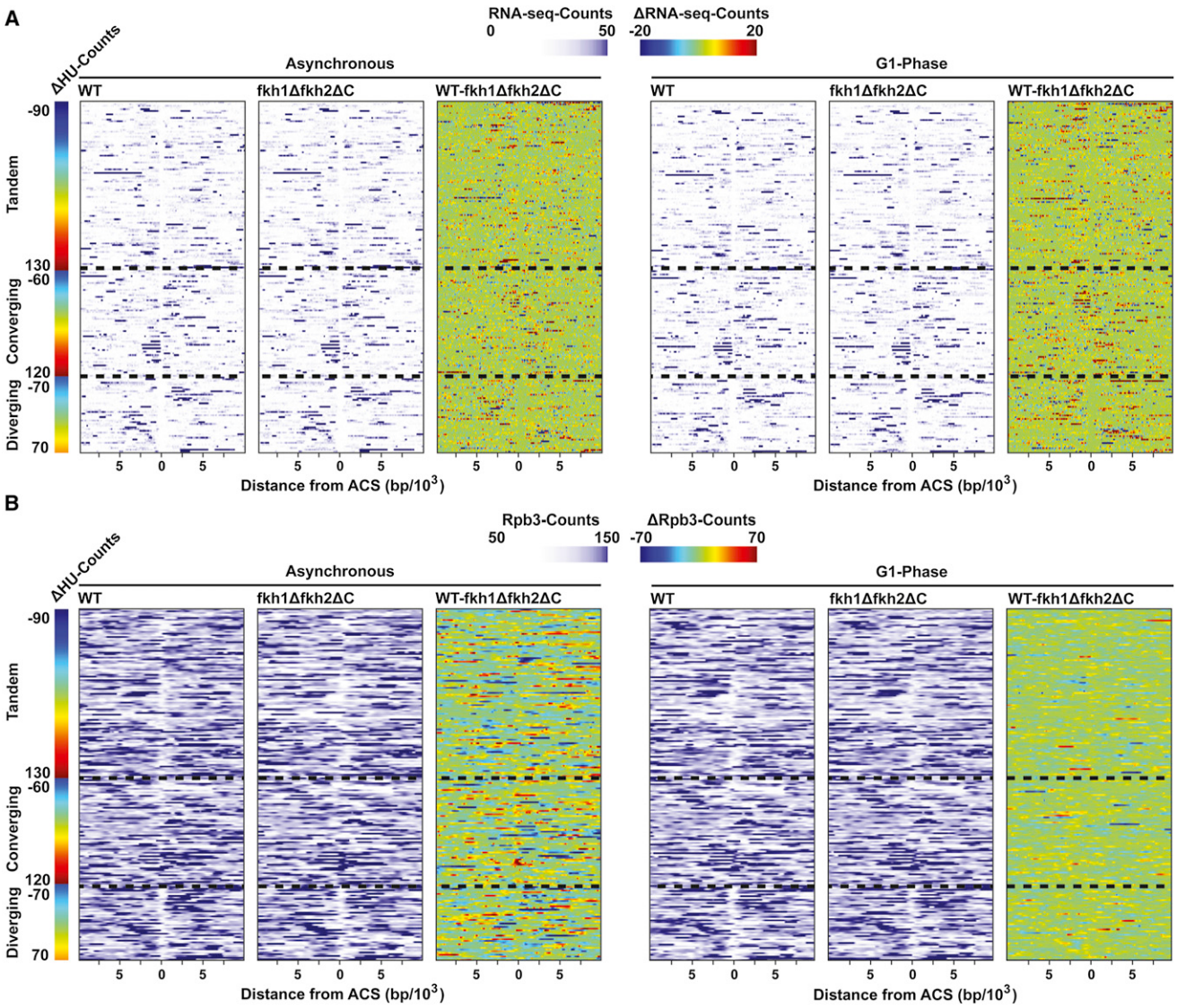

Figure 4. Transcription Analysis Surrounding Fkh-Regulated Origins in Unsynchronized and G1-Synchronized Cells

RNA-Seq (A) and Rpb3 ChIP-Seq (B) read counts of WT, *fkh1Δfkh2ΔC*, and *WT-fkh1Δfkh2ΔC* differences (Δ), within 10 kb of each Fkh-regulated origin, are aligned by each origin's predicted or verified ACS. Origins are grouped according to the orientation of the flanking genes, and arranged by differences (*WT-fkh1Δfkh2ΔC*) in BrdU incorporation in HU (ΔHU Counts). See also Table S2.

Fkh-Dependent Origin Regulation Is Not Correlated with Transcription Levels or Changes

The notion of a mechanistic link between replication origin timing and transcriptional state, together with the well-characterized roles of Fkh1 and Fkh2 as transcriptional regulators, suggested that altered transcription, particularly of genes proximal to Fkh-regulated origins, might explain the altered origin firing. Although expression of Fkh2ΔC suppressed pseudohyphal growth, indicating that normal transcriptional regulation had been at least partially restored, we nonetheless wished to determine whether differences in transcription of genes proximal to the affected origins could account for the differences in origin activity. Accordingly, we analyzed global RNA transcript levels using strand-specific RNA quantification by sequencing (RNA-Seq) and RNA Polymerase II (Pol II) occupancy using chromatin immunoprecipitation analyzed by sequencing (ChIP-Seq) of the Pol II core subunit Rpb3 in WT and *fkh1Δfkh2ΔC* cells, in unsynchronized cells and cells synchronized in G1 phase, when replication timing is established (Dimitrova and Gilbert, 1999; Raghuraman et al., 1997). Upregulation of *CLB2* in G1 phase *fkh1Δfkh2ΔC* cells, which is consistent with the role of Fkh1 in *CLB2* repression, and significant overlap between genes identified by the different methods validated both analyses (Table S2). A permutation test indicates that genes deregulated in *fkh1Δfkh2ΔC* cells are not significantly colocalized with or proximal to Fkh-regulated origins (see Experimental Procedures). We

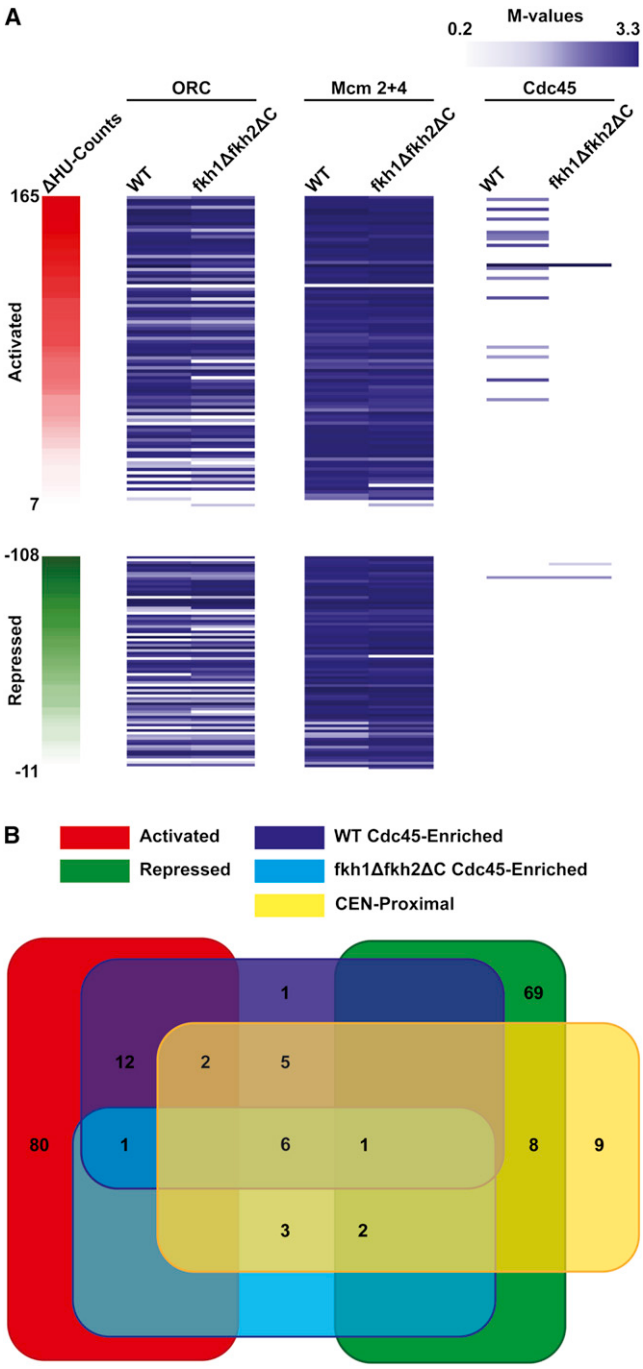

Figure 5. Genome-wide Binding of Replication Initiation Factors to Fkh-Regulated Origins

(A) M values from ChIP-chip analysis of ORC, Mcm2+4, and Cdc45 at Fkh-regulated origins (in rows) are arranged by differences (*WT-fkh1Δfkh2ΔC*) in BrdU incorporation in HU (ΔHU Counts).

(B) Venn diagram of Cdc45 binding within different origin classes is shown. See also Table S3.

also plotted RNA transcript levels and Rpb3 occupancy, as well as their differences in *fkh1Δfkh2ΔC* cells, within 10 kb of Fkh-regulated origins (Figure 4). Visual inspection of these plots show no obvious correlation with the effects on origin activities, regardless of the magnitude or directionality (positive or negative) of effect, the orientation of the immediately flanking genes, or the cell cycle stage. Linear regression analysis also shows no consistent correlation between the effects on origin activity and the expression levels of the immediately flanking genes (see Experimental Procedures). These findings demonstrate that origin regulation by Fkh1/2 does not involve proximal changes in transcription.

Cdc45 Preferentially Associates with Fkh-Activated Origins in G1 Phase

We wondered whether Fkh1/2 regulate replication timing by modulating the binding of replication factors to origins. To determine whether Fkh1/2 influence ORC binding or MCM loading, we used ChIP analyzed by microarray (ChIP-chip) to examine ORC binding in unsynchronized cells and Mcm2+4 binding in G1-synchronized cells. The results show no significant, global difference in ORC or Mcm2+4 origin-binding between WT and *fkh1Δfkh2ΔC* cells (Figure 5A and Table S3), contrary to the idea that Fkh1/2 affect origin-firing by modulating ORC or MCM binding.

Origin initiation requires the DDK-dependent recruitment of Cdc45 to pre-RCs. However, Cdc45 associates specifically, albeit relatively weakly, with several early replication origins in G1 phase (prior to DDK activation), presaging their characteristic early S phase activity (Aparicio et al., 1999). This suggests that these origins gain an early advantage (by G1 phase) in their ability to recruit Cdc45 to enable early initiation. Examination of Cdc45 binding by ChIP-chip shows Cdc45 association with many early origins, including Fkh-activated origins, such as *ARS305* and *ARS607*, and a number of CEN-proximal origins (Figures 5A and 5B and Table S3). Of 28 origins that bind Cdc45 in WT G1 phase cells, 15 are Fkh-activated and 14 are CEN-proximal (on 11 CENs), while only one is Fkh-repressed. Strikingly, in the *fkh1Δfkh2ΔC* cells, Cdc45 binding is lost from the Fkh-activated origins, which become significantly later firing, leaving only 13 origins binding Cdc45 (Figure 5B and Table S3). Of these 13, 12 are CEN-proximal, which as shown above, remain early firing. Thus, Cdc45 origin-binding in G1 phase is robustly associated with early initiation. These findings support the idea that Fkh1/2 influence origin function by regulating access to the pool of replication factors such as Cdc45, whereas CEN-proximal origins have access to Cdc45 independently of Fkh1/2.

Fkh1/2 Are Required for Selective Clustering of Fkh-Activated Origins in G1 Phase

The organization of selected origins into subnuclear domains or replication foci by Fkh1/2 may explain their preferential access to limiting or sequestered initiation factors like Cdc45. In accord with this, a global analysis of intra- and inter-chromosomal interactions of the yeast genome using a variation of 4C (chromosome conformation capture-on-chip) suggests that early origins cluster in G1 phase (Duan et al., 2010). We analyzed these origin interaction data to determine whether origin clustering was associated with Fkh regulation and/or Cdc45 binding in G1 phase. Two-dimensional clustering based on origin interaction frequencies resulted in two main clusters of interacting origins, with 89 and 92

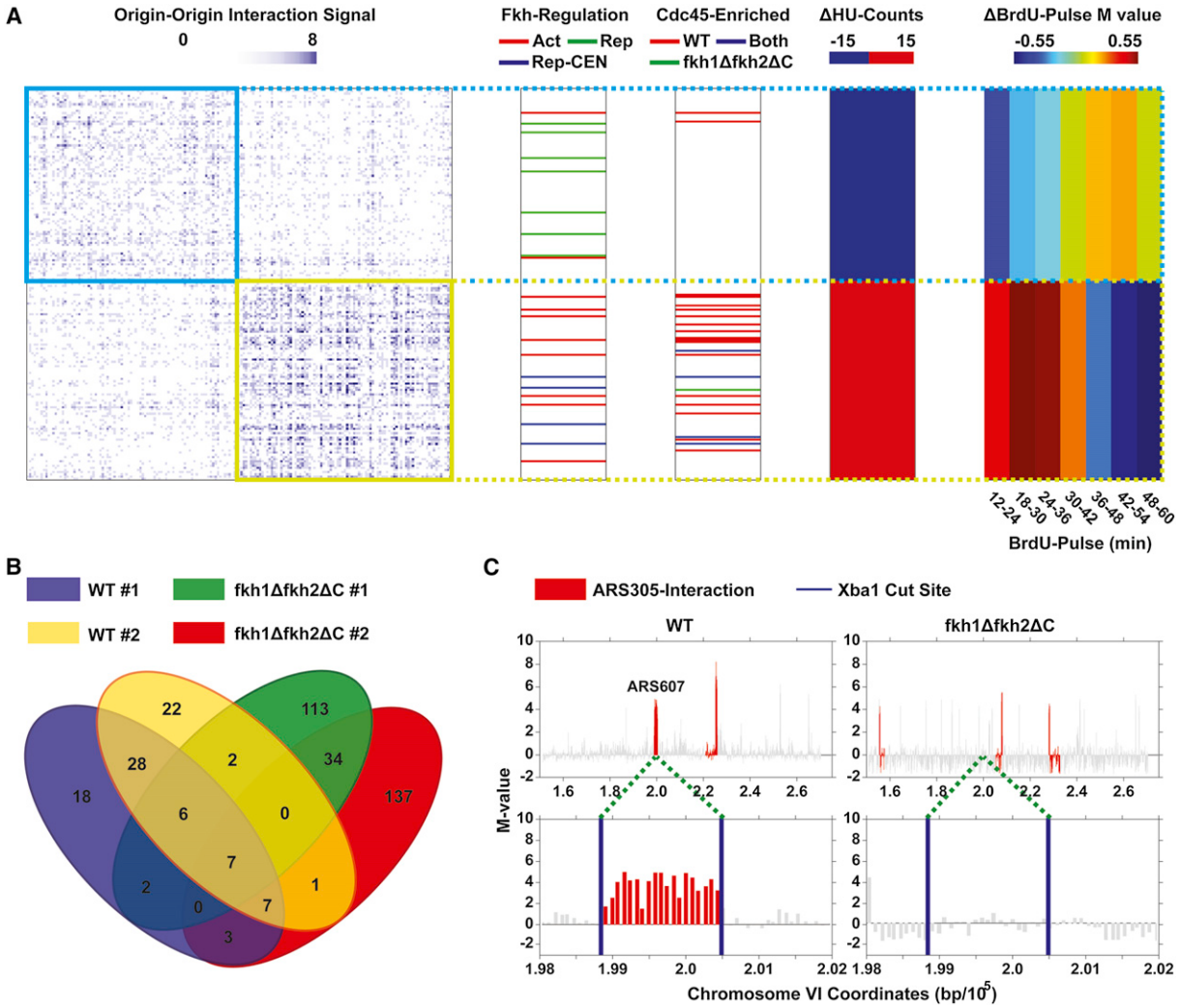

Figure 6. Chromosome-Conformation Capture Analyses of Origin Interactions

(A) Two-dimensional clustering of origin-origin interaction frequencies is shown, with origins in columns and rows of the matrix. Columns to the right indicate Cdc45 ChIP-chip binding, average BrdU ΔHU-counts, and ΔBrdU-pulse M values. The top 5% (based on p values) of Fkh-activated and Fkh-repressed origins are indicated.

(B) Venn diagram of overlap between experimental replicates is shown.

(C) Plots of the *ARS607* region including relevant *XbaI* sites are shown.

See also Figure S3 and Table S4.

origins, respectively (Figure 6A). One cluster contains most of the Cdc45-bound origins, the most statistically significant Fkh-activated origins, and CEN-proximal origins. This cluster also contains earlier-firing origins on average than the other main cluster and is depleted of non-CEN proximal, Fkh-repressed origins (hypergeometric test, $p < 0.005$). These findings suggest that Fkh regulation involves selective origin clustering.

To test whether Fkh1/2 have a role in origin clustering, we used 4C to analyze the *trans* associations of Fkh-activated origin *ARS305* with other genomic sequences (for scheme, see Figure S3A). We validated this analysis by comparing overlap between experimental replicates of WT and mutant cells, with and without crosslinking, and by analyzing the number of intra- versus inter-chromosomal interactions detected (Figure S3B). As expected, and consistent with the results of (Duan et al., 2010), intrachromosomal interactions were enriched versus interchromosomal interactions ($p < 0.001$). We detected 48 *ARS305*-interacting loci in both WT replicates (of 71 and 72 in the replicates), and 41 *ARS305*-interacting loci in both *fkh1Δfkh2ΔC* replicates (of 164 and 189 in the replicates) (Figure 6B and Table S4). The larger number of detected interactions with lower overlap between them in the *fkh1Δfkh2ΔC* replicates is consistent with a decrease in specificity of *ARS305* interactions in the mutant cells. Most of the 48 sites in WT cells were not detected in the mutant cells, indicating that their interaction with *ARS305* is Fkh1/2-dependent. For example, *ARS305* interacted with *ARS607* (as shown previously (Duan et al., 2010)) in both WT replicates and in neither *fkh1Δfkh2ΔC* replicate (Figure 6C),

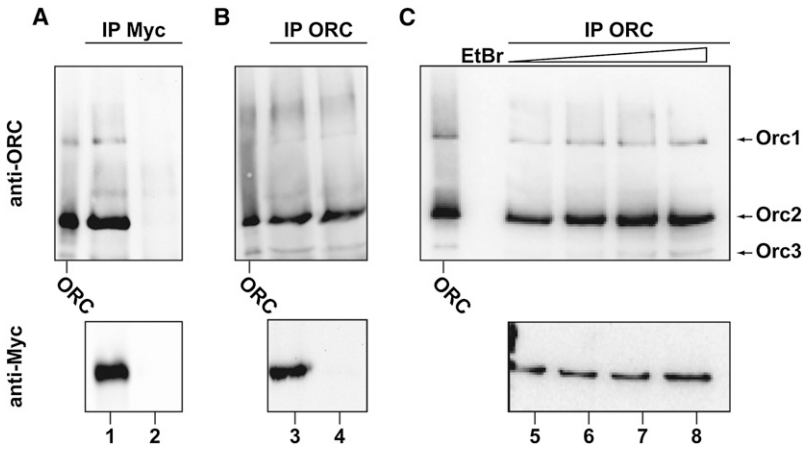

Figure 7. Co-IP of Fkh1 with ORC

Soluble extracts from *FKH1-MYC* (lanes 1, 3, and 5–8) and untagged (lanes 2 and 4) cells were subjected to IP with anti-Myc antibody (A) and anti-ORC antibody (B) and (C). IPs were analyzed by immunoblotting with anti-Myc and anti-ORC antibodies. (C) Ethidium bromide (EtBr) was included in the IPs at 10, 40, and 100 μg/mL in lanes 6, 7, and 8, respectively. ORC protein was included as standard.

indicating that Fkh1/2 are required for interaction in G1 phase between these early-firing, Fkh-activated origins. These results indicate that Fkh1/2 play a role in determining the long-range chromatin contacts made by *ARS305*, and support the idea that Fkh1/2 function in origin regulation through origin clustering.

Fkh1 and Fkh2 Interact with ORC

The binding of Fkh1/2 adjacent to many Fkh-activated origins, including *ARS305* and *ARS607* (data not shown and Harbison et al., 2004; Keich et al., 2008), led us to hypothesize that Fkh1/2 bound near origins might stabilize origin contacts in *trans* through interaction with ORC bound at other Fkh-activated origins. Immunoprecipitation (IP) of Myc-tagged Fkh1 or Fkh2 from soluble cell extracts resulted in coprecipitation of ORC (Figure 7A, lanes 1 and 2, data not shown for Fkh2); Orc2 was robustly detected, Orc1 and Orc3 were weakly detected, and Orc4-Orc6 were obscured by comigrating immunoglobulin heavy chain (data not shown). Reciprocal IP of ORC using a polyclonal antibody coprecipitated Fkh1 (Figure 7B, lanes 3 and 4). Taken together, these results demonstrate a physical interaction (direct or indirect) between ORC and Fkh1. These interactions persisted in the presence of the DNA-intercalating agent, ethidium bromide, indicating that the interactions are likely not DNA-mediated (Figure 7C, lanes 5–8). Together with the close proximity of Fkh1/2 binding sites with origin ACSs, these results support the idea that Fkh1/2 interact with ORC to bridge replication origins in *trans*.

DISCUSSION

Fkh1/2 Establish Replication-Timing Domains through Origin Clustering

Our findings reveal a novel, global mechanism for the regulation of origin initiation timing, involving the spatial organization of replication origins by Fkh1/2. Previous studies have concluded that yeast origins are early by default, and that late timing is imposed by flanking sequences of a repressive nature (Ferguson and Fangman, 1992; Friedman et al., 1996). However, our findings show that Fkh1/2 actively program the timing of most of the earliest origins throughout the genome. Thus, we propose that Fkh1/2 establish early replication timing at Forkhead-activated origins by recruiting these origins into clusters where Cdc45 is (and likely other replication factors are) concentrated. The enrichment and distinct positioning relative to the ACS of Fkh1/2 binding sites likely explains the selective preference for Fkh-activated origins. Clustering may involve interaction of Fkh1/2 bound adjacent to an origin with ORC bound to a distal, second origin. Likewise, Fkh1/2 bound near the second origin might interact with a third origin, and so forth, providing a mechanism to cluster several origins together. This congregation of origins and initiation factors provides a kinetic advantage in assembling the factors needed for replication initiation upon S phase entry, which transforms these origin clusters into early replication factories. The ensuing dynamics of the replication process, involving spooling of DNA through the replication factories (Kitamura et al., 2006), eventually repositions more distal, unfired origins, bringing them in proximity of the concentration of the replication factor(ie)s and thereby allowing them to gain access as early replicons terminate and are released. This is expected to result in an increasingly stochastic pattern of replication initiation as S phase proceeds and many unfired origins compete for limited access. However, later-replicating regions also exhibit well-defined replication patterns indicating preferred origin timing and usage. Indeed, chromosomes IV, XII, XIV, and XV each have distinctly late-replicating regions > 200 kb in length, encompassing groups of contiguous Fkh-repressed origins, which lose this unique character in the absence of Fkh1/2 (Figure 2A and Data S2).

Origin clusters may define replication-timing domains. The organization of mammalian chromosomes into spatial domains correlates strongly with replication timing (Ryba et al., 2010). Analysis of global 4C in yeast shows clustering of early origins (in G1 phase), and we have now shown that the early origin cluster contains Fkh-activated and Cdc45-bound origins (in G1 phase). We have confirmed that Fkh-activated origins *ARS305* and *ARS607* interact in *trans*, and critically, show that this interaction depends on Fkh1/2. In addition, Fkh-activated and Fkh-repressed origins often occur in separate, linearly contiguous groups along chromosomes, suggesting the formation of distinct domains. This may involve the anchoring of intrachromosomal chromatin loops by Fkh1/2 bound near origins, perhaps through interaction with ORC, particularly in the case of Fkh-activated origins, which are enriched for Fkh1/2 binding. In the case of Fkh-repressed origins, a dearth of Fkh1/2 binding sites presumably reduces the likelihood that these origins join the

Fkh-activated clusters, which may permit other mechanisms, such as deacetylation or localization to the nuclear periphery, to define replication timing of these regions. Alternatively, the later timing may be a consequence of conformational or spatial constraints imposed by the chromosomal architecture established by Fkh1/2 clustering of Fkh-activated origins.

In the absence of Fkh1 and Fkh2, CEN-proximal origins dominate the early replication landscape, suggesting that CENs confer early replication intrinsically. CENs normally cluster and occupy a characteristic interior position in the nucleus (Jin et al., 1998) that we suggest overlaps with the pool of replication factor(ie)s. Consequently, CEN-proximal origins have favorable access to this pool and initiate early, independently of Fkh1/2. Thus, CEN-proximal origins may act as organizing sites for early-replicating origin clusters that include non-CEN-proximal origins. More distal Fkh-activated origins may utilize Fkh1/2 to cluster with CEN-proximal origins, thereby drawing these more distal origins into the pool. This is consistent with the finding that CEN-proximal origins localize to the large, early-replicating cluster in the global 4C data together with the earliest Fkh-activated origins. Thus, the advanced replication timing of CEN-proximal origins (and perhaps other Fkh-repressed origins) in cells lacking Fkh1/2 may result from reduced competition from Fkh-activated origins for limiting replication factor(ie)s, rather than a direct repressive function of Fkh1/2. Incidentally, CEN-proximity may explain the finding in yeast that plasmid-borne origins typically replicate early, as these studies were performed with CEN-harboring plasmids (Ferguson and Fangman, 1992; Friedman et al., 1996).

In contrast to CENs, TELs form several clusters that occupy the nuclear periphery (Gotta et al., 1996; Heun et al., 2001). The normally late replication of TEL-proximal regions is consistent with the notion that the dynamic nature of the replication process eventually relocates these distal regions to the interior of the nucleus, which ultimately enables their access to replication factor(ie)s. In the absence of Fkh1 and Fkh2, most of the active telomeric origins are further delayed. We imagine that the delayed activation of Fkh-activated origins located along distal chromosomal arms results in a corresponding delay in the relocation to TEL-proximal origins to the vicinity of replication factor(ie)s. Alternatively, Fkh1/2 may act directly to regulate TEL-proximal origins. Further study will be required to understand the regulation of CEN- and TEL-proximal origin timing.

Multiple, Separable Roles for Fkh1 and Fkh2 in Regulation of the Genome

A clear finding of this study is the mechanistic independence of Fkh-origin regulation from transcription. There is no correlation between the observed changes in replication timing and transcriptional levels of proximal genes. Importantly, expression of Fkh2 lacking its C terminus in *fkh1*Δ*fkh2*Δ cells significantly restores transcriptional regulation of *CLB2* cluster genes (only *CLB2* remained deregulated and only in G1 phase cells) without restoring origin regulation, directly demonstrating a separation of these Fkh1/2 functions. Nevertheless, our results do not rule out the possibility that the function of Fkh1/2 in origin clustering may also underlie transcriptional control not elicited under our growth conditions.

As transcriptional regulators, Fkh1 and Fkh2 exhibit opposing, as well as partially complementary functions (Murakami et al., 2010). Fkh1 and Fkh2 also demonstrate distinct abilities to regulate origins, suggesting that the features that distinguish Fkh1 and Fkh2 functions in transcription also impinge on their functions as origin regulators. Whereas Fkh2 plays the lead role in transcriptional regulation, Fkh1 plays the lead role in origin regulation. Fkh1 differs from Fkh2 most significantly in the presence of a C-terminal extension in Fkh2, which regulates its interaction(s) with transcriptional coactivator(s) (Darieva et al., 2010, 2003; Koranda et al., 2000; Pic-Taylor et al., 2004; Reynolds et al., 2003). This domain is also required for Fkh2's function in origin regulation, suggesting that proper regulation of coactivator interactions is critical, and that factors interacting with Fkh2 but not with Fkh1 may disrupt origin regulation. Mcm1, which binds cooperatively with Fkh2, but not Fkh1 (Boros et al., 2003; Koranda et al., 2000; Kumar et al., 2000; Pic et al., 2000), is an intriguing candidate, as it has been reported to modulate origin function (Chang et al., 2004). We note that Mcm1 binding sites are not enriched near Fkh-activated origins (data not shown). Thus, consistent with the lack of effect on origin firing of *FKH2* deletion, it is possible that Fkh2 normally plays no role in origin regulation, and only substitutes (partially) in Fkh1's absence.

Fkh1, but not Fkh2, also regulates donor preference in yeast mating-type switching (Sun et al., 2002). Mating-type switching involves homologous recombination between the *MAT* locus (recipient) and one of two silent mating-type loci (donor) distally located on opposite arms of the same chromosome, *HML*α and *HMRa*. This mechanism presumably necessitates chromosomal looping of either arm to juxtapose the donor and recipient loci. Remarkably, in *MATa* cells, *HML*α is preferentially selected as the donor in over 90% of cells, which ensures efficient mating-type switching. This preference depends on Fkh1 binding to the recombination enhancer (RE), which is proximal to *HML*α. Our finding that Fkh1/2 mediate long-range origin interactions suggest that Fkh1 mediates a stable, long-range interaction between *MATa* and the RE to specify the recombination between *MATa* and *HML*α, which conspicuously, like early origin clustering, occurs during G1 phase. The role of Fkh1 in regulating recombination over long distances together with Fkh1/2's role in regulating replication initiation timing through long-range origin clustering suggests that establishing long-range chromatin contacts may be a common mechanism of Fkh1/2 function, likely extending to transcriptional control.

Our proposed mechanism of origin clustering may also explain how the long-range interaction necessary for recombinational donor preference is established. Dormant origins are closely associated with the RE (*ARS304*) and with *MAT* (*ARS313* and *ARS314*). Thus, interactions between Fkh1 bound to the RE and ORC bound to the distal *ARS313* or *ARS314* may stabilize long-range contacts between these loci; similar interactions between ORC bound to *ARS304* and Fkh1 bound near *MAT* may also participate (though an RE-like element has not been identified near *MAT*). The dormancy of these origins is consistent with the idea that these loci form a separate chromosomal domain dedicated for recombination, which delays replication (by inhibiting initiation and allowing passive replication from

distal, flanking origins). Exactly how such domains are dedicated to one function over another will require more investigation, but may reflect combinatorial regulation by Fkh1/2 together with other factors, along with defined sub-nuclear localization of these activities.

The findings presented here provide a clearer understanding of the epigenetic basis for differential origin regulation and its connection to the spatial organization of chromosomes. Rather than a direct connection with transcription, the results indicate that the organization of origins into functional clusters determines their activation kinetics. Our study identifies Fkh1 and Fkh2 as factors that participate in the establishment of the three-dimensional structure of the yeast genome and the epigenetic regulation of genome replication. This regulation through structure may be analogous to epigenetic mechanisms of transcriptional memory wherein gene looping or sub-nuclear localization is correlated with the maintenance of a transcriptional state or a potentiated state primed for rapid response (Misteli, 2007). Furthermore, this organization may contribute to a coordination of replication and transcription, perhaps with consequence for genome stability (Knott et al., 2009a). Indeed, this study's findings provide a new handle to investigate the consequences of deregulating replication timing on gene regulation or genome stability. The identification of yeast members of the conserved Fox transcription factor family as physical mediators of chromosomal architecture and epigenetic regulation suggest conservation of this function, which may link replication timing control and the role of Fox proteins in metazoan development.

EXPERIMENTAL PROCEDURES

Additional details are given in the Extended Experimental Procedures.

Yeast Strains and Methods

W303-derived, BrdU-incorporating strains were used for all strain constructions (Viggiani and Aparicio, 2006). Cell cycle block-and-release, DNA content analysis, and two-dimensional gel analysis have been described (Aparicio et al., 2004). Co-IP was performed as described (Hu et al., 2008), except Dynabeads Protein G (Invitrogen) was used. BrdU-labeled DNA was isolated as described (Viggiani et al., 2010); salmon sperm DNA was omitted for sequencing. 80 ng of BrdU-IPed DNA was prepared for single-end sequencing by Illumina ChIP-Seq protocol or 10 ng of BrdU-IPed DNA was prepared for hybridization to microarrays as described (Viggiani et al., 2010). ChIP-chip was performed and analyzed as described (Knott et al., 2009b; Viggiani et al., 2009). ChIP-Seq was performed identically except that culture was scaled-up 4-fold to generate 5–10 ng of IP material for single-end sequencing by Illumina ChIP-Seq protocol. RNA was isolated from 20 mL cultures using RiboPure Yeast Kit (Ambion). rRNA was depleted with Ribominus Beads (Invitrogen), and purified RNA was prepared for strand-specific RNA-Seq as described in (Parkhomchuk et al., 2009). We used a custom microarray design (Nimblegen) that tiles one ~60 bp oligonucleotide for every ~80 bp of unique genomic sequence. For hybridization and washing we followed Nimblegen protocols, and for image capture used an Axon 4100A Scanner.

Preprocessing of Sequence Data

Sequencing was carried out with an Illumina GAII. BrdU-IP-Seq and ChIP-Seq were analyzed with 36 bp single-end reads, while RNA-Seq was analyzed with 36 bp paired-end reads. Reads were aligned to *S. cerevisiae* genome release r.64 with PerM (Chen et al., 2009), allowing only unique matches with a maximum of two mismatches per end. BrdU-IP-Seq and Rpb3 ChIP-Seq reads were binned into nonoverlapping 50 bp bins; bin-counts were median-smoothed (1000 bp and 500 bp windows, respectively) and quantile-normalized across all experiments. This smoothing step was repeated. For all other gene expression analysis, each RNA-Seq read was assigned to a gene only when at least one of its paired-ends was fully contained within the gene's ORF and when the read's orientation corresponded to the gene's orientation. Reads whose paired-ends mapped to two or more genes were discarded. Gene read-counts were quantile-normalized prior to differential expression analysis.

Analysis of Linear Clustering of Fkh-Regulated Origins

We performed Monte Carlo simulations to determine the likelihood of the observed level of clustering between like-regulated origins (e.g., both Fkh-activated) along the chromosome occurring by chance. In each simulation we randomly assigned (from 352 total origins) 95 origins as Fkh-activated and 80 as Fkh-repressed (on each simulation) and determined the number of occurrences where two Fkh-repressed or -activated origins neighbored each other. We then compared the observed level of such instances to the empirical distribution obtained through simulations to calculate a p value.

Analysis of Fkh1 and Fkh2 Binding Sites

To determine whether Fkh1 and Fkh2 are differentially bound at Fkh-regulated versus Fkh-unregulated origins we used the *p*osition-*w*eight *m*atrices (PWMs) defined in (Morozov and Siggia, 2007) to identify all putative Fkh1/2 binding sites near origins (PWM-score cutoff = 5.5). We defined Fkh1/2-bound origins as those with a putative site within 500 bp of its BrdU-peak apex. To determine the distribution of Fkh1/2 binding sites relative to ACSs, for each Fkh1/2-bound origin with a defined ACS, we calculated the distance from the ACS to the highest scoring binding site (ACS locations from Eaton et al., 2010); we applied a kernel density function to these distances to define the probability curves.

Analysis of Global 4C

226 origins whose defined regions (as listed in OriDB) were fully contained within an *EcoRI* and a *HindIII* restriction fragment were analyzed. The restriction fragment interaction map from (Duan et al., 2010) was used to build two-dimensional interaction matrices for each restriction fragment set containing the 226 origins. The matrix value (0 to 4) represents the interaction distance between two origin-containing restriction fragments defined in (Duan et al., 2010). The two matrices were summed and the two-dimensional clustering algorithm defined in (Duan et al., 2010) was applied. 17 clusters containing fewer than ten origins each (45 total) were not analyzed further.

ACCESSION NUMBERS

All original and processed data files can be found at http://www.ncbi.nlm.nih.gov/geo/ under accession number GSE33704.

SUPPLEMENTAL INFORMATION

Supplemental Information includes Extended Experimental Procedures, two data files, four tables, and three figures and can be found with this article online at doi:10.1016/j.cell.2011.12.012.

ACKNOWLEDGMENTS

We thank: J. Aparicio, M. Arbeitman, C. Fox, and M. Michael for critical evaluation of the manuscript; M. Arbeitman for sharing equipment; S.P. Bell for purified ORC and antibody; L. Chen for valuable insight; J. Dalton for help with microscopy; C. Fox for plasmids, strains, antibody, and helpful discussion; R. Kalhor for the 4C protocol and invaluable advice; U. Keich for helpful discussion; and M. Hampsey, D. Kowalski and R. Young for strains. This work was funded by a pilot grant from the USC Epigenome Center sponsored by the Whittier Foundation (to O.M.A), NIH grants 5R01-GM065494 and 3R01-GM065494-S1(to O.M.A.), and P50-HG02790 (to S.R.V.K. and S.T.).

Received: July 14, 2011
Revised: October 11, 2011
Accepted: December 9, 2011
Published: January 19, 2012

REFERENCES

Aggarwal, B.D., and Calvi, B.R. (2004). Chromatin regulates origin activity in Drosophila follicle cells. Nature *430*, 372–376.

Aparicio, J.G., Viggiani, C.J., Gibson, D.G., and Aparicio, O.M. (2004). The Rpd3-Sin3 histone deacetylase regulates replication timing and enables intra-S origin control in Saccharomyces cerevisiae. Mol. Cell. Biol. *24*, 4769–4780.

Aparicio, O.M., Stout, A.M., and Bell, S.P. (1999). Differential assembly of Cdc45p and DNA polymerases at early and late origins of DNA replication. Proc. Natl. Acad. Sci. USA *96*, 9130–9135.

Bell, S.P., and Dutta, A. (2002). DNA replication in eukaryotic cells. Annu. Rev. Biochem. *71*, 333–374.

Boros, J., Lim, F.L., Darieva, Z., Pic-Taylor, A., Harman, R., Morgan, B.A., and Sharrocks, A.D. (2003). Molecular determinants of the cell-cycle regulated Mcm1p-Fkh2p transcription factor complex. Nucleic Acids Res. *31*, 2279–2288.

Cadoret, J.C., Meisch, F., Hassan-Zadeh, V., Luyten, I., Guillet, C., Duret, L., Quesneville, H., and Prioleau, M.N. (2008). Genome-wide studies highlight indirect links between human replication origins and gene regulation. Proc. Natl. Acad. Sci. USA *105*, 15837–15842.

Chang, V.K., Donato, J.J., Chan, C.S., and Tye, B.K. (2004). Mcm1 promotes replication initiation by binding specific elements at replication origins. Mol. Cell. Biol. *24*, 6514–6524.

Chen, Y., Souaiaia, T., and Chen, T. (2009). PerM: efficient mapping of short sequencing reads with periodic full sensitive spaced seeds. Bioinformatics *25*, 2514–2521.

Danis, E., Brodolin, K., Menut, S., Maiorano, D., Girard-Reydet, C., and Mechali, M. (2004). Specification of a DNA replication origin by a transcription complex. Nat. Cell Biol. *6*, 721–730.

Darieva, Z., Clancy, A., Bulmer, R., Williams, E., Pic-Taylor, A., Morgan, B.A., and Sharrocks, A.D. (2010). A competitive transcription factor binding mechanism determines the timing of late cell cycle-dependent gene expression. Mol. Cell *38*, 29–40.

Darieva, Z., Pic-Taylor, A., Boros, J., Spanos, A., Geymonat, M., Reece, R.J., Sedgwick, S.G., Sharrocks, A.D., and Morgan, B.A. (2003). Cell cycle-regulated transcription through the FHA domain of Fkh2p and the coactivator Ndd1p. Curr. Biol. *13*, 1740–1745.

Diller, J.D., and Raghuraman, M.K. (1994). Eukaryotic replication origins: control in space and time. Trends Biochem. Sci. *19*, 320–325.

Dimitrova, D.S., and Gilbert, D.M. (1999). The spatial position and replication timing of chromosomal domains are both established in early G1 phase. Mol. Cell *4*, 983–993.

Duan, Z., Andronescu, M., Schutz, K., McIlwain, S., Kim, Y.J., Lee, C., Shendure, J., Fields, S., Blau, C.A., and Noble, W.S. (2010). A three-dimensional model of the yeast genome. Nature *465*, 363–367.

Eaton, M.L., Galani, K., Kang, S., Bell, S.P., and MacAlpine, D.M. (2010). Conserved nucleosome positioning defines replication origins. Genes Dev. *24*, 748–753.

Eaton, M.L., Prinz, J.A., MacAlpine, H.K., Tretyakov, G., Kharchenko, P.V., and MacAlpine, D.M. (2011). Chromatin signatures of the Drosophila replication program. Genome Res. *21*, 164–174.

Ferguson, B.M., and Fangman, W.L. (1992). A position effect on the time of replication origin activation in yeast. Cell *68*, 333–339.

Flanagan, J.F., and Peterson, C.L. (1999). A role for the yeast SWI/SNF complex in DNA replication. Nucleic Acids Res. *27*, 2022–2028.

Friedman, K.L., Diller, J.D., Ferguson, B.M., Nyland, S.V., Brewer, B.J., and Fangman, W.L. (1996). Multiple determinants controlling activation of yeast replication origins late in S phase. Genes Dev. *10*, 1595–1607.

Gilbert, D.M. (2002). Replication timing and transcriptional control: beyond cause and effect. Curr. Opin. Cell Biol. *14*, 377–383.

Gondor, A., and Ohlsson, R. (2009). Replication timing and epigenetic reprogramming of gene expression: a two-way relationship? Nat. Rev. Genet. *10*, 269–276.

Goren, A., Tabib, A., Hecht, M., and Cedar, H. (2008). DNA replication timing of the human beta-globin domain is controlled by histone modification at the origin. Genes Dev. *22*, 1319–1324.

Gotta, M., Laroche, T., Formenton, A., Maillet, L., Scherthan, H., and Gasser, S.M. (1996). The clustering of telomeres and colocalization with Rap1, Sir3, and Sir4 proteins in wild-type Saccharomyces cerevisiae. J. Cell Biol. *134*, 1349–1363.

Harbison, C.T., Gordon, D.B., Lee, T.I., Rinaldi, N.J., Macisaac, K.D., Danford, T.W., Hannett, N.M., Tagne, J.B., Reynolds, D.B., Yoo, J., et al. (2004). Transcriptional regulatory code of a eukaryotic genome. Nature *431*, 99–104.

Heun, P., Laroche, T., Raghuraman, M.K., and Gasser, S.M. (2001). The positioning and dynamics of origins of replication in the budding yeast nucleus. J. Cell Biol. *152*, 385–400.

Hiratani, I., Takebayashi, S., Lu, J., and Gilbert, D.M. (2009). Replication timing and transcriptional control: beyond cause and effect–part II. Curr. Opin. Genet. Dev. *19*, 142–149.

Hollenhorst, P.C., Pietz, G., and Fox, C.A. (2001). Mechanisms controlling differential promoter-occupancy by the yeast forkhead proteins Fkh1p and Fkh2p: implications for regulating the cell cycle and differentiation. Genes Dev. *15*, 2445–2456.

Hu, F., Gan, Y., and Aparicio, O.M. (2008). Identification of Clb2 residues required for Swe1 regulation of Clb2-Cdc28 in Saccharomyces cerevisiae. Genetics *179*, 863–874.

Hu, Y.F., Hao, Z.L., and Li, R. (1999). Chromatin remodeling and activation of chromosomal DNA replication by an acidic transcriptional activation domain from BRCA1. Genes Dev. *13*, 637–642.

Jenuwein, T., and Allis, C.D. (2001). Translating the histone code. Science *293*, 1074–1080.

Jin, Q., Trelles-Sticken, E., Scherthan, H., and Loidl, J. (1998). Yeast nuclei display prominent centromere clustering that is reduced in nondividing cells and in meiotic prophase. J. Cell Biol. *141*, 21–29.

Karnani, N., Taylor, C.M., Malhotra, A., and Dutta, A. (2010). Genomic study of replication initiation in human chromosomes reveals the influence of transcription regulation and chromatin structure on origin selection. Mol. Biol. Cell *21*, 393–404.

Keich, U., Gao, H., Garretson, J.S., Bhaskar, A., Liachko, I., Donato, J., and Tye, B.K. (2008). Computational detection of significant variation in binding affinity across two sets of sequences with application to the analysis of replication origins in yeast. BMC Bioinformatics *9*, 372.

Kitamura, E., Blow, J.J., and Tanaka, T.U. (2006). Live-cell imaging reveals replication of individual replicons in eukaryotic replication factories. Cell *125*, 1297–1308.

Knott, S.R., Viggiani, C.J., and Aparicio, O.M. (2009a). To promote and protect: coordinating DNA replication and transcription for genome stability. Epigenetics *4*, 362–365.

Knott, S.R., Viggiani, C.J., Aparicio, O.M., and Tavaré, S. (2009b). Strategies for analyzing highly enriched IP-chip datasets. BMC Bioinformatics *10*, 305.

Knott, S.R., Viggiani, C.J., Tavaré, S., and Aparicio, O.M. (2009c). Genome-wide replication profiles indicate an expansive role for Rpd3L in regulating replication initiation timing or efficiency, and reveal genomic loci of Rpd3 function in Saccharomyces cerevisiae. Genes Dev. *23*, 1077–1090.

Koranda, M., Schleiffer, A., Endler, L., and Ammerer, G. (2000). Forkhead-like transcription factors recruit Ndd1 to the chromatin of G2/M-specific promoters. Nature *406*, 94–98.

Kumar, R., Reynolds, D.M., Shevchenko, A., Goldstone, S.D., and Dalton, S. (2000). Forkhead transcription factors, Fkh1p and Fkh2p, collaborate with Mcm1p to control transcription required for M-phase. Curr. Biol. *10*, 896–906.

Li, R., Yu, D.S., Tanaka, M., Zheng, L., Berger, S.L., and Stillman, B. (1998). Activation of chromosomal DNA replication in Saccharomyces cerevisiae by acidic transcriptional activation domains. Mol. Cell. Biol. *18*, 1296–1302.

Lipford, J.R., and Bell, S.P. (2001). Nucleosomes positioned by ORC facilitate the initiation of DNA replication. Mol. Cell *7*, 21–30.

MacAlpine, D.M., and Bell, S.P. (2005). A genomic view of eukaryotic DNA replication. Chromosome Res. *13*, 309–326.

MacAlpine, H.K., Gordan, R., Powell, S.K., Hartemink, A.J., and MacAlpine, D.M. (2010). Drosophila ORC localizes to open chromatin and marks sites of cohesin complex loading. Genome Res. *20*, 201–211.

MacIsaac, K.D., Wang, T., Gordon, D.B., Gifford, D.K., Stormo, G.D., and Fraenkel, E. (2006). An improved map of conserved regulatory sites for Saccharomyces cerevisiae. BMC Bioinformatics *7*, 113.

Marahrens, Y., and Stillman, B. (1992). A yeast chromosomal origin of replication defined by multiple functional elements. Science *255*, 817–823.

Mechali, M. (2010). Eukaryotic DNA replication origins: many choices for appropriate answers. Nat. Rev. Mol. Cell Biol. *11*, 728–738.

Meister, P., Taddei, A., Ponti, A., Baldacci, G., and Gasser, S.M. (2007). Replication foci dynamics: replication patterns are modulated by S-phase checkpoint kinases in fission yeast. EMBO J. *26*, 1315–1326.

Miotto, B., and Struhl, K. (2007). Med. Sci. (Paris) *23*, 735–740.

Misteli, T. (2007). Beyond the sequence: cellular organization of genome function. Cell *128*, 787–800.

Morozov, A.V., and Siggia, E.D. (2007). Connecting protein structure with predictions of regulatory sites. Proc. Natl. Acad. Sci. USA *104*, 7068–7073.

Murakami, H., Aiba, H., Nakanishi, M., and Murakami-Tonami, Y. (2010). Regulation of yeast forkhead transcription factors and FoxM1 by cyclin-dependent and polo-like kinases. Cell Cycle *9*, 3233–3242.

Pappas, D.L., Jr., Frisch, R., and Weinreich, M. (2004). The NAD(+)-dependent Sir2p histone deacetylase is a negative regulator of chromosomal DNA replication. Genes Dev. *18*, 769–781.

Parkhomchuk, D., Borodina, T., Amstislavskiy, V., Banaru, M., Hallen, L., Krobitsch, S., Lehrach, H., and Soldatov, A. (2009). Transcriptome analysis by strand-specific sequencing of complementary DNA. Nucleic Acids Res. *37*, e123.

Pic, A., Lim, F.L., Ross, S.J., Veal, E.A., Johnson, A.L., Sultan, M.R., West, A.G., Johnston, L.H., Sharrocks, A.D., and Morgan, B.A. (2000). The forkhead protein Fkh2 is a component of the yeast cell cycle transcription factor SFF. EMBO J. *19*, 3750–3761.

Pic-Taylor, A., Darieva, Z., Morgan, B.A., and Sharrocks, A.D. (2004). Regulation of cell cycle-specific gene expression through cyclin-dependent kinase-mediated phosphorylation of the forkhead transcription factor Fkh2p. Mol. Cell. Biol. *24*, 10036–10046.

Raghuraman, M.K., Brewer, B.J., and Fangman, W.L. (1997). Cell cycle-dependent establishment of a late replication program. Science *276*, 806–809.

Reynolds, D., Shi, B.J., McLean, C., Katsis, F., Kemp, B., and Dalton, S. (2003). Recruitment of Thr 319-phosphorylated Ndd1p to the FHA domain of Fkh2p requires Clb kinase activity: a mechanism for CLB cluster gene activation. Genes Dev. *17*, 1789–1802.

Ryba, T., Hiratani, I., Lu, J., Itoh, M., Kulik, M., Zhang, J., Schulz, T.C., Robins, A.J., Dalton, S., and Gilbert, D.M. (2010). Evolutionarily conserved replication timing profiles predict long-range chromatin interactions and distinguish closely related cell types. Genome Res. *20*, 761–770.

Sequeira-Mendes, J., Diaz-Uriarte, R., Apedaile, A., Huntley, D., Brockdorff, N., and Gomez, M. (2009). Transcription initiation activity sets replication origin efficiency in mammalian cells. PLoS Genet. *5*, e1000446.

Sporbert, A., Gahl, A., Ankerhold, R., Leonhardt, H., and Cardoso, M.C. (2002). DNA polymerase clamp shows little turnover at established replication sites but sequential de novo assembly at adjacent origin clusters. Mol. Cell *10*, 1355–1365.

Stevenson, J.B., and Gottschling, D.E. (1999). Telomeric chromatin modulates replication timing near chromosome ends. Genes Dev. *13*, 146–151.

Sun, K., Coic, E., Zhou, Z., Durrens, P., and Haber, J.E. (2002). Saccharomyces forkhead protein Fkh1 regulates donor preference during mating-type switching through the recombination enhancer. Genes Dev. *16*, 2085–2096.

Unnikrishnan, A., Gafken, P.R., and Tsukiyama, T. (2010). Dynamic changes in histone acetylation regulate origins of DNA replication. Nat. Struct. Mol. Biol. *17*, 430–437.

Viggiani, C.J., Aparicio, J.G., and Aparicio, O.M. (2009). ChIP-chip to analyze the binding of replication proteins to chromatin using oligonucleotide DNA microarrays. Methods Mol. Biol. *521*, 255–278.

Viggiani, C.J., and Aparicio, O.M. (2006). New vectors for simplified construction of BrdU-Incorporating strains of Saccharomyces cerevisiae. Yeast *23*, 1045–1051.

Viggiani, C.J., Knott, S.R., and Aparicio, O.M. (2010). Genome-wide analysis of DNA synthesis by BrdU immunoprecipitation on tiling microarrays (BrdU-IP-chip) in Saccharomyces cerevisiae. Cold Spring Harb Protoc *2010*, pdb prot5385.

Vogelauer, M., Rubbi, L., Lucas, I., Brewer, B.J., and Grunstein, M. (2002). Histone acetylation regulates the time of replication origin firing. Mol. Cell *10*, 1223–1233.

Weber, J.M., Irlbacher, H., and Ehrenhofer-Murray, A.E. (2008). Control of replication initiation by the Sum1/Rfm1/Hst1 histone deacetylase. BMC Mol. Biol. *9*, 100.

Weinreich, M., Palacios DeBeer, M.A., and Fox, C.A. (2004). The activities of eukaryotic replication origins in chromatin. Biochim. Biophys. Acta *1677*, 142–157.

Cell

EXTENDED EXPERIMENTAL PROCEDURES

Yeast Strain and Plasmid Constructions

W303-derived, BrdU-incorporating strains CVy43 (*Mata ade2-1, bar1::hisG, can1-100, his3-11,15, leu2-3,112, trp1-1, ura3-1::BrdU-Inc::URA3*) or CVy63 (*Mata ade2-1, bar1::hisG, can1-100, his3-11,15, leu2-3,112, trp1-1, leu2::BrdU-Inc::LEU2*) were the WT parents for all strain constructions (Viggiani and Aparicio, 2006). *FKH1* and *FKH2* were deleted in CVy43 as described (Longtine et al., 1998), yielding strains: ZOy1 (*fkh1Δ::kanMX6*), CVy138 (*fkh2Δ::His3MX6*), and CVy139 (*fkh1Δ::kanMX6 fkh2Δ::His3MX6*); only differences in genotype from CVy43 are indicated. Plasmid pfkh2ΔC contains a C-terminally truncated *NotI-KpnI* fragment of *FKH2* (truncated at the native *KpnI* site in *FKH2*, deleting amino acids 624–862; this maintains the entire DNA binding domain and all homology with Fkh1) into pRS424 digested with the same enzymes; pfkh2ΔC was transformed into CVy139 yielding strain SKy1. *CDC45-HA3* (*LEU2*) was introduced into strains CVy43 and CVy139 + pfkh2ΔC using p405-CDC45-HA/C as described (Aparicio et al., 1997), yielding strains CVy46 and T2y3, respectively. *FKH1-MYC9* replaced *FKH1* in CVy138 using plasmid pTOPO-Fkh1-Myc9, yielding strain ZOy22. pTOPO-Fkh1-Myc9 was constructed using Phusion High-Fidelity PCR kit (New England Biolabs, M0530) to amplify *FKH1-MYC9-TRP1* from genomic DNA of strain Z1448 (Harbison et al., 2004), and inserting it into pCR2.1-TOPO vector (Invitrogen).

Strain ARy23 containing mutations of two Fkh1/2 binding sites at *ARS305* was constructed by pop-in/pop-out of plasmid p306-ARS305-Δ2BS into strain CVy63 and confirmed by sequencing of PCR-amplified genomic DNA. Plasmid p306-ARS305Δ2BS was constructed as follows: Two ~1 kb fragments covering *ARS305* with overlapping ends were amplified from genomic DNA (using primers: 5′-gtcaagcttggcaatgtcaagagcagagc with 5′-gtcctcgaggaatacataacaaaaatataaaaacc for one fragment and 5′-tgagaatt-caggcatcagtttgatgttgg with 5′-gtcctcgaggtccctttaattttaggatatgaaaac for the second fragment), digested with *EcoRI* +*XhoI* and with *XhoI* + *HindIII*, respectively, and three-way ligated into pRS306 digested with *EcoRI* + *HindIII*. The *XhoI* site changes the first predicted Fkh1/2 binding site (chr III coordinates 39,563-39,570) without deleting or inserting additional sequence. The resulting plasmid, p306-ARS305Δ1BS was sequenced to confirm that only the desired sequence changes were introduced. This plasmid was mutagenized using QuikChange Lightning Multi Site mutagenesis kit (Agilent# 210515-5) using primer (5′-caaagaaaaaaatct-tagctttaagaactacaaagtcctcgaggaataataaatcacaccggacagtacatg) to change the second predicted Fkh1/2 binding site (chr III coordinates 39,483-39,490) to an *XhoI* site without deleting or inserting additional sequence. The resulting plasmid p306-ARS305Δ2BS was sequenced to confirm that only the desired sequence changes were introduced.

Antibody Methods

For BrdU and chromatin IPs we used: anti-BrdU at 1:1000 (GE Healthcare, RPN202), anti-Fkh1 at 1:200 (Casey et al., 2008), anti-ORC at 1:500 (Wyrick et al., 2001), anti-Mcm2 at 1:50 (Santa Cruz Biotech., SC-6680), anti-Mcm4 at 1:50 (Santa Cruz Biotech., SC-33622), anti-Ha 16B12 at 1:200 (Covance, MMS101R), and anti-Rpb3 at 1:500 (Neoclone, W0012). We used anti-Myc 9E10 at 1:100 and 1:2000 (Covance, MMS150P), and anti-ORC at 1:100 and 1:1000, for co-IP and immunoblotting, respectively.

BrdU-IP-Seq Analysis

To identify an initial set of peaks in each experiment, a set of apices (bins whose count was higher than any neighboring bin within 500 bp) were detected. We assigned a magnitude to these peaks equal to the number of reads mapping to within 500 bp of the apex; only peaks with a magnitude > 10 were considered further. For each strain we aligned replicate apex chromosomal locations using the dynamic programming algorithm as described (Knott et al., 2009), with a gap penalty of 1000 bp. Apices that did not align across all replicates were removed from consideration. Next, for each strain we aligned peaks (387) with the set of previously annotated origins listed in OriDB (Nieduszynski et al., 2007); peaks (35) that did not align to an annotated origin were not considered further.

Origins that were not detected to incorporate BrdU within a given strain were assigned a count equal to the number of reads that mapped to within 500 bp of the average of its corresponding detected apices. To test for differential BrdU-incorporation across strains, we employed DESeq (Anders and Huber, 2010). Origin counts were normalized using DESeq's internal size and variance normalization strategies and were called as different between two strains with a significance cutoff of FDR < 0.005.

BrdU-IP-Chip Time-Course Data Analysis

Due to the high proportion of enriched probes in BrdU-IP-chip experiments, within-array normalization methods designed for ChIP-chip are not suitable (Knott et al., 2009). To compensate for this, we developed a procedure and tested it on BrdU-IP-chip experiments performed in the presence of HU. This method requires that un-enriched probes form a dense cluster in the M = log(IP/Total) versus A = (log(IP)+log(Total))/2 plane (Knott et al., 2009). However, in BrdU incorporation experiments without HU (where the percentage of enriched probes can reach 80%), this requirement is sometimes not met. To account for this, we developed a technique specifically for such experiments. This method requires a mock control, for which we hybridized BrdU-IP material obtained from a 12 min BrdU pulse using G1-arrested (nonreplicating) cells against genomic DNA. First, we identified the best axes on which to transform the experimental data by applying our previous method on the control data (Knott et al., 2009). After transforming the control and experimental data onto these axes, the median absolute deviations of both datasets were normalized to 1. Then, the M values of the experimental data were location-normalized such that mean of the lowest 20% of probes were equal to mean of the lowest 20% of control probes. Subsequently, we followed our previous method (Knott et al., 2009).

Analysis of Linear Clustering of Fkh-Regulated Origins

To test whether Fkh-activated and –repressed origins cluster in separate groups linearly along chromosomes, we defined a clustering metric equal to the number of "cuts" required to separate Fkh-repressed and Fkh-activated origins (this is equivalent to the number of instances where a Fkh-activated origin neighbors a Fkh-repressed origin, ignoring non-Fkh-regulated origins). A low "cut" count indicates higher clustering of like-regulated origins. We obtained a "cut" count of 65 in the experimental data. To test if this was significantly low, we performed 10^6 simulations on the 352 origins that were detected in WT or *fkh1*Δ*fkh2*Δ*C* cells. In each simulation we randomly assigned 95 origins as Fkh-activated, 80 as Fkh-repressed, and the remaining as Fkh-unregulated. Fewer than 1% of the simulations resulted in a "cut" count < 65 (Figure S2D).

Analysis of Fkh-Regulated Transcription versus Fkh-Regulated Origin Function

To determine whether proximal genes show coregulation with Fkh-regulated origins, we performed a permutation test on the distances between Fkh-regulated origins and the nearest Fkh-regulated genes. Fkh-regulated genes were identified as those that showed differential expression (DESeq FDR < 0.01) between WT and *fkh1*Δ*fkh2*Δ*C* cells in the same condition (unsynchronized or G1-synchronized). This analysis was performed using both the RNA-Seq and Rpb3-ChIP-Seq datasets, (genes detected as differentially expressed in each of the experiments are listed in Table S1). For each experiment we calculated the distance from each Fkh-regulated origin to the nearest Fkh-regulated gene's promoter. Next, 10^5 simulated origin sets were identified by randomly selecting 172 origins, and randomly assigning 95 as Fkh-activated and 82 as Fkh-repressed. For each of these sets, the minimum distances to the nearest Fkh-regulated genes were calculated. With this analysis we determined for all possible pair-wise combinations (e.g., upregulated gene and Fkh-activated origin, downregulated gene and Fkh-activated origin, etc.) that Fkh-regulated origins are not significantly clustered with Fkh-regulated genes along the chromosome.

To test for correlation of Fkh-regulated origins with flanking gene expression, we performed regression analysis separately on Fkh-regulated origins lying within intergenic regions flanked by diverging, converging, and tandemly oriented genes. For converging and diverging intergenic regions, we used two covariates representing the unsynchronized and G1 phase *fkh1*Δ*fkh2*Δ*C-WT* RNA-Seq read count differences of the closest transcript (as measured in bp between the origin's ARS-consensus sequence (ACS) and the gene's nearest end) and two covariates representing the same difference measure in the farther of the two transcripts. For tandem intergenic regions, two covariates represented unsynchronized and G1 phase *fkh1*Δ*fkh2*Δ*C-WT* RNA-Seq read count differences for the converging gene and another two covariates represented the differences for the diverging gene. In this analysis the only covariate that showed significant correlation with origin regulation was the gene farthest away from origins within converging intergenic regions in unsynchronized cells ($p < 0.05$). A closer inspection revealed that this correlation was due to four outlying data points, and when these were removed, the same analysis found no covariate to be significantly correlated with origin regulation. Furthermore, the application of this same analysis to read count differences in the Rpb3 ChIP-Seq data showed no covariate to be significantly predictive of origin regulation.

Chromosome Conformation Capture on Chip (4C)

Chromatin Isolation

50 mL of G1-sychronized cells were crosslinked and harvested as described for ChIP-chip (Viggiani et al., 2009). Cells were suspended in 9.5 mL Buffer Z (0.7M Sorbitol, 50 mM Tris [pH 7.4], heat sterilized) plus freshly added 2-mercaptoethanol (20 mM final) and protease inhibitor cocktail (Roche, Mini Complete). 0.5mL Zymolyase 100T (ICN, 10 mg/mL freshly made in Buffer Z) was added and the suspension was incubated at 30°C with gentle agitation, 35 min. The suspension was split into six 2 mL microcentrifuge tubes and centrifuged at 16,000 × *g*, 20 min at 4°C. The supernatants were discarded, each pellet was suspended in 300 μL NP buffer (1 M Sorbitol, 100 mM Tris [pH 7.4], 50 mM NaCl, 5 mM $MgCl_2$, 1 mM $CaCl_2$, heat sterilized) containing 0.5 mM Spermidine (freshly added from 250 mM stock) by gently pipetting with a wide-bore pipet tip, and the samples were pooled in a 2mL microcentrifuge tube.

Digestion and Ligation I

The suspension was centrifuged as above and the pellet was suspended in 500 μL ice-cold 1X NEB (New England Biolabs) digestion buffer II, and centrifuged again. This wash step with digestion buffer was repeated and the pellet was suspended in 50 μL 1X NEB digestion buffer II. 42μL 1% SDS was added, mixed gently, incubated at 60°C, 15 min. 328 μL of ice-cold 1X NEB digestion buffer II was added and the resulting suspension was centrifuged at 600 × *g*, 1 min at 4°C. 400 μL of the supernatant was transferred to a fresh microcentrifuge tube (the remainder was discarded), and 44 μL 10% Triton X-100 was added and mixed gently by pipetting with a wide-bore pipet tip. This suspension was placed on ice for 15 min, after which 58.4 μL of H_2O, 16 μL 10X NEB digestion buffer II, and 1.6 μL BSA (NEB, 10 mg/mL) were added.

4 μL *XbaI* (NEB, 100 U/μL) was added, mixed gently, and incubated at 37°C for a minimum of 8 hr while shaking at 275 rpm. 10 μL H_2O, 50 μL 10% SDS, and 9 μL 0.5 M EDTA was added, mixed, and incubated at 65°C for 10 min, followed by 60°C for 10 min, and on ice for 5 min. The sample was transferred to a 15mL conical screw-cap tube on ice and 3554 μL H_2O, 250 μL 10X T4 DNA ligase buffer (NEB), 50 μL BSA (10 mg/mL), 500 μL 10% Triton X-100, and 125 μL 1M Tris (pH 7.5) were added, mixed gently, and incubated on ice, 15 min. While on ice, 2 μL T4 DNA ligase (NEB, 400 U/μL) was added, mixed gently, and incubated at 16°C for 4 hr, after which 60 μL 0.5 M EDTA was added.

To the ligated sample, 50 μL 5M NaCl and 5 μL RNAase A (20 mg/mL) were added, mixed, and incubated at 37°C, 1 hr. 25 μL Proteinase K (20 mg/mL) was added, mixed, and incubated overnight at 65°C. The sample was transferred to a 15 mL phase-lock tube (5-Prime, 2302850) and the DNA was purified by extraction with 6 mL phenol:chloroform:isoamyl alcohol (25:24:1) and centrifugation according to the manufacturer's instructions. To the 4.2 mL of aqueous solution recovered, 225 μL 5 M NaCl and 6 μL glycoblue were added and mixed, and 11 mL of ice-cold ethanol was added, mixed, and incubated at −20°C, 8 hr. The sample was aliquoted into eight 2 mL microcentrifuge tubes and centrifuged at ~16,000 g, 30 min at 4°C. After discarding the supernatant, each pellet was dissolved in 50 μL 1X TE and the samples were pooled. 30 μL 3 M NaOAc (pH 5.2) and 825 μL of ice-cold ethanol were added, mixed, and incubated at −80°C, 2 hr. The precipitate was recovered by centrifugation at 16,000 × *g*, 30 min at 4°C, and after discarding the supernatant, the pellet was dissolved in 50 μL TE.

Digestion and Ligation II

To 25 μL (~100ng) of the ligated sample, 64 μL H_2O, 10 μL 10X NEB digestion buffer II, 1 μL BSA (10 mg/mL, NEB) were added and mixed, and 2 μL of *MseI* (10 U/μL, NEB) was added, mixed, and incubated at 37°C, 2 hr. 1 μL 20% SDS was added and incubated at 65°C, 20 min; 30 μL 10% Triton X-100 was added and incubated on ice for 15 min. 757 μL H_2O, 100 μL T4 DNA ligase buffer, and 10 μL BSA (10 mg/mL) were added and incubated on ice for 15 min. While still on ice, 2 μL T4 DNA Ligase (400 U/μL) was added, mixed by pipetting gently, and incubated overnight at 16°C. The sample was split into two 500 μL aliquots (in 2 mL microcentrifuge tubes) and 25 μL 5 M NaCl, 2 μL glycoblue, and 1.2 mL ice-cold ethanol was added to each, mixed and incubated at −20°C, 2 hr. The precipitate was recovered by centrifugation at 16,000 × *g*, 30 min at 4°C; the supernatant was discarded and each pellet was dissolved in 25 μL TE and pooled.

Amplification and Microarray Analysis

5 μL was amplified by standard PCR (25 cycles) with the following primers: 5′CTAAGTGTCCTGTTTCGGAAC, and 5′CAGGCCGC TCTTATAAAATGA. 1μg amplified DNA was labeled with Cy5 and hybridized against Cy3-labeled reference DNA (G1-synchronized total genomic DNA) as described for BrdU-IP-chip (Viggiani et al., 2010). Analysis was performed as described in (Knott et al., 2009) to identify enriched probes, and *Xba1* fragments containing > 3 enriched probes immediately adjacent to either cut site were deemed to be interacting.

SUPPLEMENTAL REFERENCES

Anders, S., and Huber, W. (2010). Differential expression analysis for sequence count data. Genome Biol. *11*, R106.

Aparicio, O.M., Weinstein, D.M., and Bell, S.P. (1997). Components and dynamics of DNA replication complexes in S. cerevisiae: redistribution of MCM proteins and Cdc45p during S phase. Cell *91*, 59–69.

Casey, L., Patterson, E.E., Muller, U., and Fox, C.A. (2008). Conversion of a replication origin to a silencer through a pathway shared by a Forkhead transcription factor and an S phase cyclin. Mol. Biol. Cell *19*, 608–622.

Harbison, C.T., Gordon, D.B., Lee, T.I., Rinaldi, N.J., Macisaac, K.D., Danford, T.W., Hannett, N.M., Tagne, J.B., Reynolds, D.B., Yoo, J., et al. (2004). Transcriptional regulatory code of a eukaryotic genome. Nature *431*, 99–104.

Knott, S.R., Viggiani, C.J., Aparicio, O.M., and Tavaré, S. (2009). Strategies for analyzing highly enriched IP-chip datasets. BMC Bioinformatics *10*, 305.

Longtine, M.S., McKenzie, A., 3rd, Demarini, D.J., Shah, N.G., Wach, A., Brachat, A., Philippsen, P., and Pringle, J.R. (1998). Additional modules for versatile and economical PCR-based gene deletion and modification in Saccharomyces cerevisiae. Yeast *14*, 953–961.

Nieduszynski, C.A., Hiraga, S., Ak, P., Benham, C.J., and Donaldson, A.D. (2007). OriDB: a DNA replication origin database. Nucleic Acids Res. *35*, D40–D46.

Viggiani, C.J., Aparicio, J.G., and Aparicio, O.M. (2009). ChIP-chip to analyze the binding of replication proteins to chromatin using oligonucleotide DNA microarrays. Methods Mol. Biol. *521*, 255–278.

Viggiani, C.J., and Aparicio, O.M. (2006). New vectors for simplified construction of BrdU-Incorporating strains of Saccharomyces cerevisiae. Yeast *23*, 1045–1051.

Viggiani, C.J., Knott, S.R., and Aparicio, O.M. (2010). Genome-wide analysis of DNA synthesis by BrdU immunoprecipitation on tiling microarrays (BrdU-IP-chip) in Saccharomyces cerevisiae. Cold Spring Harb Protoc *2010*, pdb prot5385.

Wyrick, J.J., Aparicio, J.G., Chen, T., Barnett, J.D., Jennings, E.G., Young, R.A., Bell, S.P., and Aparicio, O.M. (2001). Genome-wide distribution of ORC and MCM proteins in S. cerevisiae: high- resolution mapping of replication origins. Science *294*, 2357–2360.

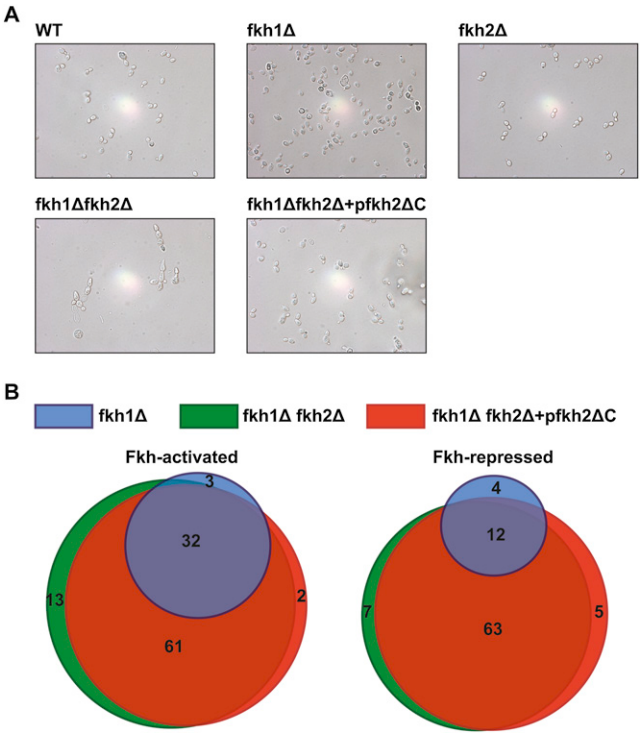

Figure S1. Related to Figure 1

(A) Suppression of pseudohyphal growth of *fkh1*Δ*fkh2*Δ cells by expression of Fkh2ΔC. Phase-contrast images of the indicated strains grown in liquid culture and sonicated mildly to disrupt cell aggregates.

(B) Origins deregulated in *fkh1*Δ, *fkh1*Δ*fkh2*Δ, and *fkh1*Δ*fkh2*Δ + *fkh2*Δ*C* cells. Venn diagrams showing overlap of deregulated origins identified as Fkh-activated and Fkh-repressed.

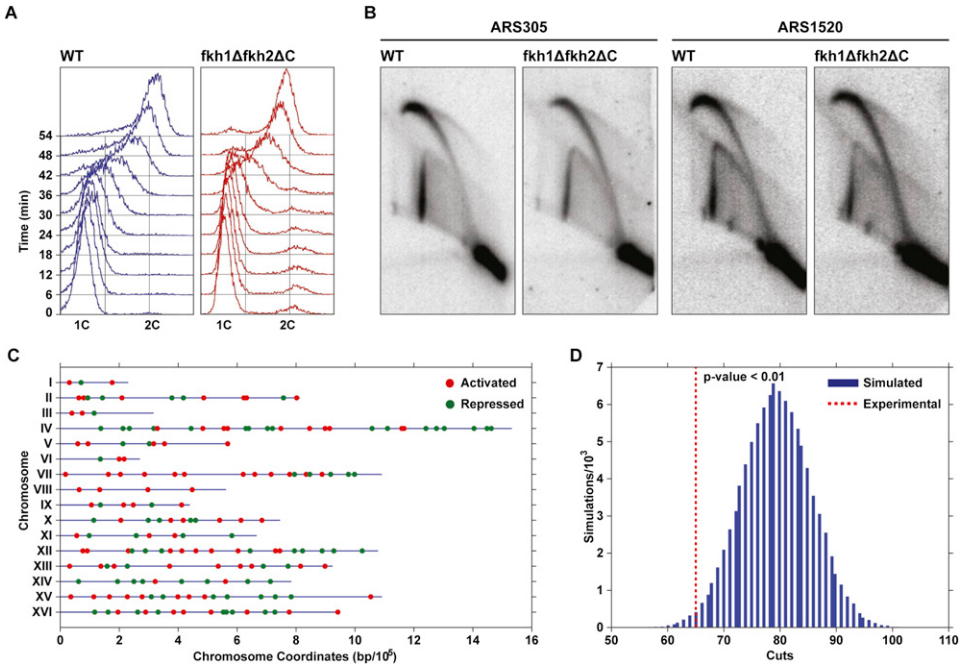

Figure S2. Related to Figure 2

(A) FACScan analysis of DNA content of WT and *fkh1Δfkh2ΔC* cells synchronized in G1 phase with α–factor and released synchronously into S phase.

(B) Two-dimensional gel electrophoresis analysis of *ARS305* (Fkh-activated) and *ARS1520* (Fkh-repressed) in unsynchronized WT and *fkh1Δfkh2ΔC* cells. Genomic DNA was digested with *NcoI* and *SalI*.

(C) Nonrandom distribution of Fkh-regulated origins. Chromosomal positions of Fhk-activated and -repressed origins are plotted.

(D) Histogram displaying the frequency of "Cut" counts observed in the 10^5 simulations as well as the experimentally observed "Cut" count. "Cuts" refers to the number of times a Fkh-activated origin is followed by a Fkh-repressed origin, or vice-versa, given a random distribution (see Experimental Procedures).

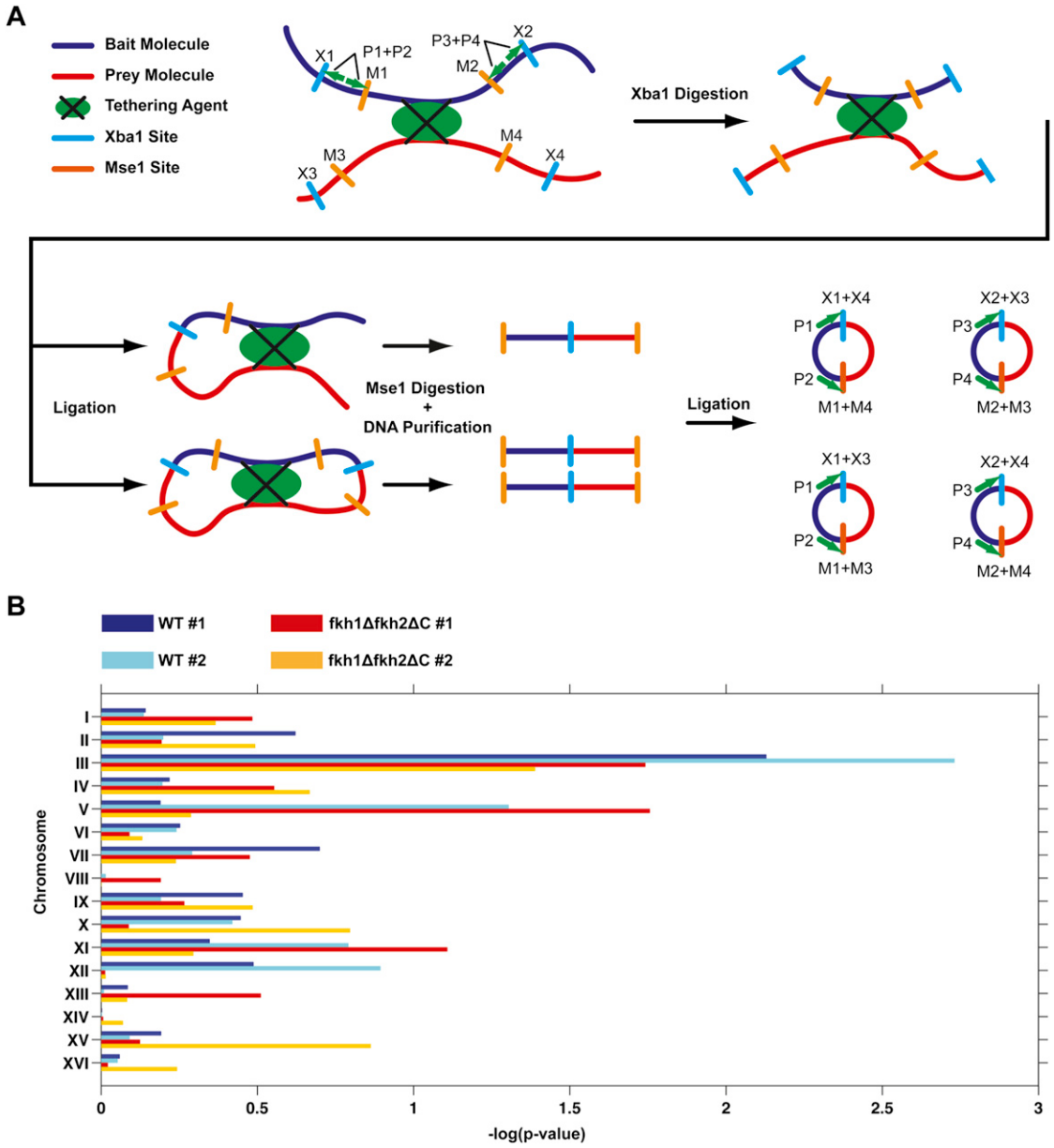

Figure S3. 4C Analysis of *ARS305* Interactions, Related to Figure 6

(A) Scheme of the 4C method showing relevant *XbaI* (X1-X4) and *MseI* (M1-M4) restriction sites surrounding *ARS305* (Bait) and a hypothetical interacting locus (Prey), and primers (P1-P4) used to amplify captured loci for identification by microarray. The tethering agent represents crosslinked protein(s) mediating interaction between the bait and prey.

(B) Statistical analysis of *ARS305* interacting sites by chromosome showing the expected preference for intrachromosomal interactions (i.e., with chromosome III). The p value is based on the number of observed versus expected interactions for each chromosome (the expected number of interactions is directly proportional to the number of *XbaI* fragments per individual chromosome).